increased expression of enterocyte CYP3A4, in the analysis of three separate cohorts (n=20, 27, and 10, respectively). However, their intestinal study populations were too small to detect differences among the *MDR1* polymorphisms by gender. Because the remarkable gender differences have been reported in the expression of CYPs and transporters (15,16), we hypothesized that the expression of CYP3A4 associated with *MDR1* genotypes would differ by gender. In the present study, we showed that *MDR1* G2677T/A-C3435T haplotypes significantly influenced the intestinal expression in women (Fig. 1). These results suggest that the *MDR1* haplotype may be a useful predictor of the inter-individual variability of the intestinal expression of CYP3A4 and the extent of some CYP3A4-mediated drug interactions in women.

The exact mechanism by which *MDR1* G2677T/A-C3435T haplotypes influence CYP3A4 expression in women remains unknown. In our results, we observed no significant difference in MDR1 mRNA expression among *MDR1* G2677T/A-C3435T haplotypes (Fig. 1 a), but it has been shown that "silent" polymorphisms (in particular, C3435T) in the *MDR1* gene can alter Pgp conformation and substrate specificity, especially when no change in MDR1 mRNA and protein levels has been reported (23). Furthermore, *in vitro* studies showed that G2677T/A-C3435T haplotypes can reduce the activity of Pgp (14). Therefore, reduced function of Pgp could possibly lead to high intracellular concentrations of endogenous regulators such as sex-steroid hormones, regulating the expression of CYP3A4 (24–27). In contrast, we found no significant differences in the hepatic expression of CYP3A4 among *MDR1* haplotypes for G2677T/A-C3435T in women. These opposing effects of the same haplotypes on hepatic and intestinal mRNA expressions of CYP3A4 in women could be partly due to differences in the underlying mechanism between the two types of organ.

Furthermore, we found that intestinal *MDR1* haplotypes had no effects on the C/D ratio of tacrolimus in LDLT patients (Table IV). Some studies have reported that 2677T or 3435T alleles affected the pharmacokinetics of tacrolimus in Caucasians (9,28,29), while others demonstrated contrary results in Asians (7,30). Similar discrepancies have been observed for digoxin (31). These might reflect disparities in different frequencies of *MDR1* haplotypes in different ethnicities (32,33). The 2677TT-3435TT haplotype is found in 42% of Caucasians and 8% of African-Americans (34), while 15.9% in the present Japanese population (Table III). Based on the present results and these previous findings, the *MDR1* haplotype is suggested to have a minor effect on the pharmacokinetics of tacrolimus in Asians compared with Caucasians.

CONCLUSION

In conclusion, the *MDR1* haplotype derived from G2677T/A and C3435T was significantly associated with intestinal CYP3A4 mRNA expression in women, but not in men, suggesting that it could be a good marker to predict the basal mRNA level of intestinal CYP3A4 in women. However, this effect was not observed for the pharmacokinetics of tacrolimus in LDLT patients. Therefore, extensive clinical pharmacokinetic studies are necessary to elucidate this effect on other drugs which are CYP3A4 substrates, in consideration of gender-differences in pharmacokinetics.

ACKNOWLEDGEMENTS

This work was supported in part by the 21st Century Center of Excellence (COE) Program "Knowledge Information Infrastructure for Genome Science", and by a grant-in-aid for Scientific Research from the Ministry of Education, Culture, Sports, Science and Technology of Japan. K. Hosohata was supported as a Research Assistant by the 21st Century COE program "Knowledge Information Infrastructure for Genome Science".

Disclosures None.

REFERENCES

1. F. Thiebaut, T. Tsuruo, H. Hamada, M. M. Gottesman, I. Pastan, and M. C. Willingham. Cellular localization of the multidrug-resistance gene product P-glycoprotein in normal human tissues. *Proc Natl Acad Sci USA*. **84**:7735–8 (1987). doi:10.1073/pnas.84.21.7735.
2. S. V. Ambudkar, S. Dey, C. A. Hrycyna, M. Ramachandra, I. Pastan, and M. M. Gottesman. Biochemical, cellular, and pharmacological aspects of the multidrug transporter. *Annu Rev Pharmacol Toxicol*. **39**:361–98 (1999). doi:10.1146/annurev.pharmtox.39.1.361.
3. Y. Kimura, S. Y. Morita, M. Matsuo, and K. Ueda. Mechanism of multidrug recognition by MDR1/ABCB1. *Cancer Sci*. **98**:1303–10 (2007). doi:10.1111/j.1349-7006.2007.00538.x.
4. S. Hoffmeyer, O. Burk, O. von Richter, H. P. Arnold, J. Brockmoller, A. Johne, I. Cascorbi, T. Gerloff, I. Roots, M. Eichelbaum, and U. Brinkmann. Functional polymorphisms of the human multidrug-resistance gene: multiple sequence variations and correlation of one allele with P-glycoprotein expression and activity *in vivo*. *Proc Natl Acad Sci USA*. **97**:3473–8 (2000). doi:10.1073/pnas.050585397.
5. U. Brinkmannand, and M. Eichelbaum. Polymorphisms in the ABC drug transporter gene MDR1. *Pharmacogenomics J*. **1**:59–64 (2001).
6. C. Marzolini, E. Paus, T. Buclin, and R. B. Kim. Polymorphisms in human MDR1 (P-glycoprotein): recent advances and clinical relevance. *Clin Pharmacol Ther*. **75**:13–33 (2004). doi:10.1016/j.clpt.2003.09.012.
7. M. Goto, S. Masuda, H. Saito, S. Uemoto, T. Kiuchi, K. Tanaka, and K. Inui. C3435T polymorphism in the MDR1 gene affects the enterocyte expression level of CYP3A4 rather than Pgp in recipients of living-donor liver transplantation. *Pharmacogenetics*. **12**:451–7 (2002). doi:10.1097/00008571-200208000-00005.
8. J. Lamba, S. Strom, R. Venkataramanan, K. E. Thummel, Y. S. Lin, W. Liu, C. Cheng, V. Lamba, P. B. Watkins, and E. Schuetz. MDR1 genotype is associated with hepatic cytochrome P450 3A4 basal and induction phenotype. *Clin Pharmacol Ther*. **79**:325–38 (2006). doi:10.1016/j.clpt.2005.11.013.
9. I. A. Macphee, S. Fredericks, T. Tai, P. Syrris, N. D. Carter, A. Johnston, L. Goldberg, and D. W. Holt. Tacrolimus pharmacogenetics: polymorphisms associated with expression of cytochrome p4503A5 and P-glycoprotein correlate with dose requirement. *Transplantation*. **74**:1486–9 (2002). doi:10.1097/00007890-200212150-00002.
10. H. Zheng, S. Webber, A. Zeevi, E. Schuetz, J. Zhang, P. Bowman, G. Boyle, Y. Law, S. Miller, J. Lamba, and G. J. Burckart. Tacrolimus dosing in pediatric heart transplant patients is related to CYP3A5 and MDR1 gene polymorphisms. *Am J Transplant*. **3**:477–83 (2003). doi:10.1034/j.1600-6143.2003.00077.x.

11. X. Zhang, Z. H. Liu, J. M. Zheng, Z. H. Chen, Z. Tang, J. S. Chen, and L. S. Li. Influence of CYP3A5 and MDR1 polymorphisms on tacrolimus concentration in the early stage after renal transplantation. *Clin Transplant.* **19**:638–43 (2005). doi:10.1111/j.1399-0012.2005.00370.x.
12. R. B. Kim, B. F. Leake, E. F. Choo, G. K. Dresser, S. V. Kubba, U. I. Schwarz, A. Taylor, H. G. Xie, J. McKinsey, S. Zhou, L. B. Lan, J. D. Schuetz, E. G. Schuetz, and G. R. Wilkinson. Identification of functionally variant MDR1 alleles among European Americans and African Americans. *Clin Pharmacol Ther.* **70**:189–99 (2001). doi:10.1067/mcp.2001.117412.
13. K. Tang, S. M. Ngoi, P. C. Gwee, J. M. Chua, E. J. Lee, S. S. Chong, and C. G. Lee. Distinct haplotype profiles and strong linkage disequilibrium at the MDR1 multidrug transporter gene locus in three ethnic Asian populations. *Pharmacogenetics.* **12**:437–50 (2002). doi:10.1097/00008571-200208000-00004.
14. N. N. Salama, Z. Yang, T. Bui, and R. J. Ho. MDR1 haplotypes significantly minimize intracellular uptake and transcellular P-gp substrate transport in recombinant LLC-PK1 cells. *J Pharm Sci.* **95**:2293–308 (2006). doi:10.1002/jps.20717.
15. A. R. Whitney, M. Diehn, S. J. Popper, A. A. Alizadeh, J. C. Boldrick, D. A. Relman, and P. O. Brown. Individuality and variation in gene expression patterns in human blood. *Proc Natl Acad Sci USA.* **100**:1896–901 (2003). doi:10.1073/pnas.252784499.
16. R. Wolbold, K. Klein, O. Burk, A. K. Nussler, P. Neuhaus, M. Eichelbaum, M. Schwab, and U. M. Zanger. Sex is a major determinant of CYP3A4 expression in human liver. *Hepatology.* **38**:978–88 (2003).
17. T. Hashida, S. Masuda, S. Uemoto, H. Saito, K. Tanaka, and K. Inui. Pharmacokinetic and prognostic significance of intestinal MDR1 expression in recipients of living-donor liver transplantation. *Clin Pharmacol Ther.* **69**:308–16 (2001). doi:10.1067/mcp.2001.115142.
18. S. Masuda, S. Uemoto, T. Hashida, Y. Inomata, K. Tanaka, and K. Inui. Effect of intestinal P-glycoprotein on daily tacrolimus trough level in a living-donor small bowel recipient. *Clin Pharmacol Ther.* **68**:98–103 (2000). doi:10.1067/mcp.2000.107912.
19. M. Yasuhara, T. Hashida, M. Toraguchi, Y. Hashimoto, M. Kimura, K. Inui, R. Hori, Y. Inomata, K. Tanaka, and Y. Yamaoka. Pharmacokinetics and pharmacodynamics of FK 506 in pediatric patients receiving living-related donor liver transplantations. *Transplant Proc.* **27**:1108–1110 (1995).
20. J. K. Lamba, Y. S. Lin, E. G. Schuetz, and K. E. Thummel. Genetic contribution to variable human CYP3A-mediated metabolism. *Adv Drug Deliv Rev.* **54**:1271–1294 (2002). doi:10.1016/S0169-409X(02)00066-2.
21. L. Wojnowski. Genetics of the variable expression of CYP3A in humans. *Ther Drug Monit.* **26**:192–199 (2004). doi:10.1097/00007691-200404000-00019.
22. T. Hirota, I. Ieiri, H. Takane, S. Maegawa, M. Hosokawa, K. Kobayashi, K. Chiba, E. Nanba, M. Oshimura, T. Sato, S. Higuchi, and K. Otsubo. Allelic expression imbalance of the human CYP3A4 gene and individual phenotypic status. *Hum Mol Genet.* **13**:2959–2969 (2004). doi:10.1093/hmg/ddh313.
23. C. Kimchi-Sarfaty, J. M. Oh, I. W. Kim, Z. E. Sauna, A. M. Calcagno, S. V. Ambudkar, and M. M. Gottesman. A "silent" polymorphism in the MDR1 gene changes substrate specificity. *Science.* **315**:525–528 (2007). doi:10.1126/science.1135308.
24. B. Goodwin, M. R. Redinbo, and S. A. Kliewer. Regulation of cyp3a gene transcription by the pregnane x receptor. *Annu Rev Pharmacol Toxicol.* **42**:1–23 (2002). doi:10.1146/annurev.pharmtox.42.111901.111051.
25. M. N. Jacobs, M. Dickins, and D. F. Lewis. Homology modelling of the nuclear receptors: human oestrogen receptorbeta (hERbeta), the human pregnane-X-receptor (PXR), the Ah receptor (AhR) and the constitutive androstane receptor (CAR) ligand binding domains from the human oestrogen receptor alpha (hERalpha) crystal structure, and the human peroxisome proliferator activated receptor alpha (PPARalpha) ligand binding domain from the human PPARgamma crystal structure. *J Steroid Biochem Mol Biol.* **84**:117–132 (2003). doi:10.1016/S0960-0760(03)00021-9.
26. J. M. Pascussi, S. Gerbal-Chaloin, L. Drocourt, P. Maurel, and M. J. Vilarem. The expression of CYP2B6, CYP2C9 and CYP3A4 genes: a tangle of networks of nuclear and steroid receptors. *Biochim Biophys Acta.* **1619**:243–253 (2003).
27. W. Y. Kimand, and L. Z. Benet. P-glycoprotein (P-gp/MDR1)-mediated efflux of sex-steroid hormones and modulation of P-gp expression *in vitro*. *Pharm Res.* **21**:1284–1293 (2004). doi:10.1023/B:PHAM.0000033017.52484.81.
28. J. Wang, A. Zeevi, K. McCurry, E. Schuetz, H. Zheng, A. Iacono, K. McDade, D. Zaldonis, S. Webber, R. M. Watanabe, and G. J. Burckart. Impact of ABCB1 (MDR1) haplotypes on tacrolimus dosing in adult lung transplant patients who are CYP3A5 *3/*3 non-expressors. *Transpl Immunol.* **15**:235–240 (2006). doi:10.1016/j.trim.2005.08.001.
29. D. Anglicheau, C. Verstuyft, P. Laurent-Puig, L. Becquemont, M. H. Schlageter, B. Cassinat, P. Beaune, C. Legendre, and E. Thervet. Association of the multidrug resistance-1 gene single-nucleotide polymorphisms with the tacrolimus dose requirements in renal transplant recipients. *J Am Soc Nephrol.* **14**:1889–1896 (2003). doi:10.1097/01.ASN.0000073901.94759.36.
30. N. Tsuchiya, S. Satoh, H. Tada, Z. Li, C. Ohyama, K. Sato, T. Suzuki, T. Habuchi, and T. Kato. Influence of CYP3A5 and MDR1 (ABCB1) polymorphisms on the pharmacokinetics of tacrolimus in renal transplant recipients. *Transplantation.* **78**:1182–1187 (2004). doi:10.1097/01.TP.0000137789.58694.B4.
31. B. Chowbay, H. Li, M. David, Y. B. Cheung, and E. J. Lee. Meta-analysis of the influence of MDR1 C3435T polymorphism on digoxin pharmacokinetics and MDR1 gene expression. *Br J Clin Pharmacol.* **60**:159–171 (2005). doi:10.1111/j.1365-2125.2005.02392.x.
32. I. Cascorbi. Role of pharmacogenetics of ATP-binding cassette transporters in the pharmacokinetics of drugs. *Pharmacol Ther.* **112**:457–473 (2006). doi:10.1016/j.pharmthera.2006.04.009.
33. C. Kimchi-Sarfaty, A. H. Marple, S. Shinar, A. M. Kimchi, D. Scavo, M. I. Roma, I. W. Kim, A. Jones, M. Arora, J. Gribar, D. Gurwitz, and M. M. Gottesman. Ethnicity-related polymorphisms and haplotypes in the human ABCB1 gene. *Pharmacogenomics.* **8**:29–39 (2007). doi:10.2217/14622416.8.1.29.
34. D. L. Kroetz, C. Pauli-Magnus, L. M. Hodges, C. C. Huang, M. Kawamoto, S. J. Johns, D. Stryke, T. E. Ferrin, J. DeYoung, T. Taylor, E. J. Carlson, I. Herskowitz, K. M. Giacomini, and A. G. Clark. Sequence diversity and haplotype structure in the human ABCB1 (MDR1, multidrug resistance transporter) gene. *Pharmacogenetics.* **13**:481–94 (2003). doi:10.1097/00008571-200308000-00006.

0090-9556/09/3704-821–826$20.00
DRUG METABOLISM AND DISPOSITION
Copyright © 2009 by The American Society for Pharmacology and Experimental Therapeutics
DMD 37:821–826, 2009

Vol. 37, No. 4
25833/3449361
Printed in U.S.A.

Impact of Intestinal *CYP2C19* Genotypes on the Interaction between Tacrolimus and Omeprazole, but Not Lansoprazole, in Adult Living-Donor Liver Transplant Patients

Keiko Hosohata, Satohiro Masuda, Toshiya Katsura, Yasutsugu Takada, Toshimi Kaido, Yasuhiro Ogura, Fumitaka Oike, Hiroto Egawa, Shinji Uemoto, and Ken-ichi Inui

Department of Pharmacy, Kyoto University Hospital (K.H., S.M., T.Kat., K.I.), and Department of Surgery, Graduate School of Medicine (Y.T., T.Kai., Y.O., F.O., H.E., S.U.), Kyoto University, Kyoto, Japan

Received November 24, 2008; accepted January 8, 2009

ABSTRACT:

To assess the effects of intestinal cytochrome P450 2C19 on the interaction between tacrolimus and proton pump inhibitors, we examined the concentration/dose ratio [(ng/ml)/(mg/day)] of tacrolimus coadministered with omeprazole (20 mg) or lansoprazole (30 mg) to 89 adult living-donor liver transplant patients on postoperative days 22 to 28, considering the *CYP2C19* genotypes of the native intestine and the graft liver, separately. The concentration/dose ratio of tacrolimus coadministered with omeprazole was significantly higher in patients with two variants (*2 or *3) for intestinal CYP2C19 (median, 6.38; range, 1.55–22.9) than intestinal wild-type homozygotes (median, 2.11; range, 1.04–2.54) and heterozygotes (median, 2.11; range, 0.52–4.33) (P = 0.010), but the extent of the increase was attenuated by carrying the wild-type allele in the graft liver even when patients were *CYP3A5*1* noncarriers. Conversely, the *CYP2C19* polymorphisms both in the native intestine and in the graft liver little influenced the interaction between tacrolimus and lansoprazole, but *CYP3A5*1* noncarriers showed higher tacrolimus concentration/dose ratio than *CYP3A5*1* carriers. Furthermore, our experiments in vitro revealed that lansoprazole had a stronger inhibitory effect on the CYP3A5-mediated metabolism of tacrolimus than omeprazole, although not significantly (IC_{50} = 19.9 ± 13.8 μM for lansoprazole, 53.7 ± 6.1 μM for omeprazole). Our findings suggest that intestinal and graft liver CYP2C19 plays a relatively greater role in the metabolism of omeprazole than it does for lansoprazole, so that the effects of CYP3A5 on the metabolism of tacrolimus might be masked by the interaction with omeprazole associated with the *CYP2C19* genotype.

The immunosuppressant tacrolimus is characterized by a narrow therapeutic index and remarkable intraindividual and interindividual variability in its pharmacokinetics (Venkataramanan et al., 1995; Kahan et al., 2002). This variability can be attributed to factors such as poor absorption (Masuda and Inui, 2006), extensive first-pass metabolism (Lampen et al., 1995; Wilkinson, 2005), and drug-drug interactions (Christians et al., 2002). Tacrolimus is mainly metabolized by cytochrome P450 (P450) 3A4 and CYP3A5 in the small intestine and liver (Shiraga et al., 1994; Hesselink et al., 2003). In particular, CYP3A5 plays a key role in the pharmacokinetics of tacrolimus (Kamdem et al., 2005; Dai et al., 2006). Several studies of heart (Zheng et al., 2003), lung (Wang et al., 2006), kidney (Haufroid et al., 2004, 2006; Macphee et al., 2005; Kuypers et al., 2007), and liver (Goto et al., 2004; Masuda et al., 2006; Uesugi et al., 2006; Fukudo et al., 2008) transplant patients treated with tacrolimus have shown a significant association between the *CYP3A5* polymorphisms and tacrolimus dose-adjusted trough blood levels.

Clinically relevant drug-drug interactions have been observed between tacrolimus and proton pump inhibitors (PPIs) in those with *CYP2C19* gene variants, poor metabolizers (PMs) and intermediate metabolizers (IMs), compared with those with no variants, extensive metabolizers (EMs) (Itagaki et al., 2004; Miura et al., 2007). Because CYP2C19 and CYP3A4/5 are mainly responsible for the metabolism of PPIs (Andersson, 1996), PPIs themselves inhibit the metabolism of tacrolimus via CYP3A4/5 in patients carrying variant alleles of *CYP2C19*, thereby increasing the blood concentrations of tacrolimus. Furthermore, the magnitude of CYP2C19-mediated metabolism of omeprazole is greater than that of lansoprazole. We have recently reported the interaction between tacrolimus and lansoprazole in a living-donor liver transplant (LDLT) patient with the *CYP2C19*2/*3* and *CYP3A5*3/*3* genotypes both in the native intestine and in the graft liver (Hosohata et al., 2008). In liver transplantation, the genetic backgrounds of the native intestine (recipient) and the graft liver (donor) are different in many cases. Furthermore, several studies have assessed the expression or catalytic activity of intestinal CYP2C19

This work was supported in part by the 21st Century Center of Excellence (COE) Program "Knowledge Information Infrastructure for Genome Science"; a grant-in-aid from the Japan Health Sciences Foundation for "Research on Health Sciences Focusing on Drug Innovation"; and a grant-in-aid for Scientific Research from the Ministry of Education, Culture, Sports, Science, and Technology of Japan.

Article, publication date, and citation information can be found at http://dmd.aspetjournals.org.

doi:10.1124/dmd.108.025833.

ABBREVIATIONS: P450, cytochrome P450; PPI, proton pump inhibitor; PM, poor metabolizer; IM, intermediate metabolizer; EM, extensive metabolizer; LDLT, living-donor liver transplantation; C/D, concentration/dose; M-I, 13-*O*-demethyl tacrolimus.

TABLE 1

Characteristics of patients (n = 89)

Data are expressed as number or mean ± S.D.

Variables	Whole (n = 89)	Treatment with PPIs	
		Omeprazole (n = 35)	Lansoprazole (n = 54)
Age, years	51.9 ± 10.3	52.4 ± 8.8	51.6 ± 11.2
Gender (male/female), n	46/43	19/16	27/27
Body weight, kg	60.0 ± 10.0	59.8 ± 10.2	60.1 ± 9.9
Graft-to-recipient weight ratio, %	1.14 ± 0.30	1.15 ± 0.29	1.13 ± 0.30
ABO blood group match (identical/compatible/incompatible), n	60/12/17	24/4/7	36/8/10
Primary disease, n			
Cirrhosis	70	30	40
Primary biliary cirrhosis	7	2	5
Fulminant hepatic failure	3	1	2
Others	9[a]	2	7
Donor age, years	45.0 ± 13.2	46.0 ± 12.6	44.3 ± 13.6
Donor gender (male/female), n	50/39	18/17	32/22

[a] The primary disease was biliary atresia, Budd-Chiari syndrome, nonalcoholic steatohepatitis, and primary sclerosing cholangitis.

(Obach et al., 2001; Lapple et al., 2003; Paine et al., 2006). Based on these backgrounds, we hypothesized that intestinal CYP2C19 would affect the interaction between tacrolimus and PPIs in liver transplant patients.

In the present study, we examined the impact of the *CYP3A5* and *CYP2C19* genotypes in the small intestine on the interaction between tacrolimus and PPIs in LDLT patients, considering the genotypes of the native intestine and the graft liver, separately. Furthermore, the inhibitory effects of the PPIs on the CYP3A5-mediated metabolism of tacrolimus were examined using recombinant microsomal preparations.

Materials and Methods

Patients. Between February 2004 and January 2008, 89 de novo adult LDLT patients and their 89 corresponding donors were enrolled in this study, having first provided their written informed consent. Patients (all Japanese) who were receiving tacrolimus with either omeprazole (n = 35) (Omepral; AstraZeneca Co. Ltd., Osaka, Japan) at 20 mg/day or lansoprazole (n = 54) (Takepron; Takeda Pharmaceutical Co. Ltd., Osaka, Japan) at 30 mg/day were studied on days 22 to 28 post-transplantation (Table 1). This study was conducted in accordance with the Declaration of Helsinki and its amendments and was approved by the Kyoto University Graduate School and Faculty of Medicine Ethics Committee.

Dosage Regimen of Tacrolimus and Measurement of Tacrolimus Concentrations. The basic immunosuppression regimen consisted of tacrolimus with low-dose steroids (Inomata et al., 1996). Tacrolimus was administered orally at a dose of 0.075 mg/kg every 12 h from the evening of postoperative day 1 (Yasuhara et al., 1995; Inomata et al., 1996). The target of the whole-blood trough concentration of tacrolimus was set at between 10 and 15 ng/ml during the first 2 weeks. Steroid treatment was started at graft reperfusion at a dose of 10 mg/kg, with a gradual reduction from 2 to 0.3 mg/kg/day during the first 2 weeks after surgery. The dosage of tacrolimus was adjusted based on whole-blood trough concentrations measured approximately 12 h after the evening dosage every day using a semiautomated microparticle enzyme immunoassay (Imx; Abbott, Tokyo, Japan) (Yasuhara et al., 1995).

Evaluation of Drug Interactions between Tacrolimus and PPIs. Because the oral administration of PPIs started approximately 2 weeks after surgery, we evaluated data on postoperative days 22 to 28. The clinical course of all the patients enrolled in this study was stable. The average of dose-normalized blood concentration of tacrolimus during this observation period then was assessed as concentration/dose (C/D) ratio [(ng/ml)/(mg/day)] of tacrolimus for each patient and used for the analysis. We excluded data obtained during treatment with a temporal high-dose steroid injection against acute cellular rejection because of induction of the intestinal expression of CYP3A4 (Masuda et al., 2004).

Genotyping. Genomic DNA was extracted from the peripheral blood of transplant patients or donors with a Wizard Genomic DNA Purification kit (Promega, Madison, WI). Because two *CYP2C19* variant alleles, *CYP2C19*2* and *CYP2C19*3*, account for the poor metabolizer phenotype in Japanese subjects (De Morais et al., 1994a), the detection of the wild-type allele (**1*) and these two variant alleles was performed using a polymerase chain reaction-restriction fragment length polymorphism method (De Morais et al., 1994a,b). The genotyping of *CYP3A5* was performed as described previously (Goto et al., 2004; Uesugi et al., 2006; Fukudo et al., 2008).

Classification of Patients. The patients themselves and their corresponding donors were separately classified into three groups based on the *CYP2C19* genotype as follows: *CYP2C19*1/*1* (EMs), *CYP2C19*1/*2* or *CYP2C19*1/*3* (IMs), and *CYP2C19*2/*2*, *CYP2C19*3/*3*, or *CYP2C19*2/*3* (PMs) (Itagaki et al., 2004). As for the *CYP3A5* genotype, patients were allocated to two groups as follows: *CYP3A5*1/*1* or *CYP3A5*1/*3* (**1* carriers) and *CYP3A5*3/*3* (**1* noncarriers).

In Vitro Inhibition of CYP3A4/5-Dependent Tacrolimus Metabolism by PPIs. To evaluate the inhibitory effects of omeprazole and lansoprazole on the metabolism of tacrolimus, we performed experiments in vitro using recombinant microsomes, as reported previously with slight modifications (Li et al., 2004; Dai et al., 2006). In brief, omeprazole and lansoprazole were serially diluted with methanol to yield final concentrations ranging from 1 to 300 μM and 1 to 200 μM, respectively. The reaction was started with 50 μl of 1.5 mM NADP (Nacalai Tesque, Kyoto, Japan) and was stopped with 1 ml of 6.25% $ZnSO_4$. The reaction mixture consisted of 400 nM tacrolimus, 12 mM glucose 6-phosphate, 0.25 IU of glucose 6-phosphate dehydrogenase, 6 mM $MgCl_2$, and 0.07 mg/ml microsomal protein for P450 (heterologous baculovirus-insect cell-expressed human CYP3A4 or human CYP3A5 in P450 reductase and cytochrome b_5) (BD Gentest, Woburn, MA) in 100 mM potassium phosphate buffer, pH 7.4, with or without PPIs, in a final volume of 500 μl. The final methanol concentration in the incubation mixture was less than 1%, with minimal impact on enzymatic activity (Li et al., 2004). The incubation conditions for CYP3A4 and CYP3A5 activities were 5 min at 37°C. The concentration of 13-*O*-demethyl tacrolimus (M-I) (a gift from Astellas Pharma Inc., Tokyo, Japan), the primary metabolite, was quantified by liquid chromatography/tandem mass spectrometry method (Shimomura et al., 2008). IC_{50} values were estimated using a nonlinear regression analysis of competition curves with one compartment, and the following equation: $V = (100 \times IC_{50})/(IC_{50} + [I]) + A$, where V is production of M-I, which accounts for most of the metabolic clearance of tacrolimus (% of control), [I] is the concentration of each PPI, and A is the nonspecific metabolism of tacrolimus (% of control).

Statistical Analysis. The C/D ratio of tacrolimus coadministered with PPIs was compared using the U test for two genotype groups or the Kruskal-Wallis test, followed by the Dunn post hoc test for multiple comparisons for more than two genotype groups. Data are expressed as the median and range or mean ± S.D., depending on data type. For all the analyses, two-tailed $P < 0.05$ was considered statistically significant. All the statistical analyses were conducted using GraphPad Prism, version 4 (GraphPad Software Inc., San Diego, CA).

TABLE 2

Effects of intestinal and graft liver CYP2C19 genotypes on the C/D ratio of tacrolimus coadministered with omeprazole (n = 35) or lansoprazole (n = 54)

Data are expressed as median (range). *CYP3A5*1* noncarriers, *CYP3A5*3/*3*. *P* values are for the differences among the genotype groups, using the Kruskal-Wallis test, followed by the Dunn post hoc test for multiple comparisons.

PPI	Variables	*CYP2C19* Genotype (*CYP3A5*1* Noncarriers)			*P*
		EMs	IMs	PMs	
Omeprazole	Native intestine				
	n	11 (9)	15 (9)	9 (9)	
	Tacrolimus C/D ratio	2.11 (1.04–2.54)	2.11 (0.52–4.33)	6.38*† (1.55–22.9)	0.010
	Graft liver				
	n	10 (6)	13 (8)	12 (7)	
	Tacrolimus C/D ratio	1.83 (1.04–6.38)	2.31 (0.52–7.10)	3.27* (1.9–22.9)	0.022
Lansoprazole	Native intestine				
	n	16 (11)	27 (21)	11 (4)	
	Tacrolimus C/D ratio	2.34 (1.16–12.8)	2.83 (0.72–13.4)	2.27 (0.98–11.7)	0.52
	Graft liver				
	n	15 (9)	30 (22)	9 (7)	
	Tacrolimus C/D ratio	2.47 (1.13–10.6)	2.76 (1.10–12.8)	2.20 (0.72–13.4)	0.82

* $P < 0.05$, EMs versus PMs; † $P < 0.05$, IMs versus PMs.

Results

Effects of Intestinal and Graft Liver *CYP2C19* Genotypes on the Interaction between Tacrolimus and PPIs. For the *CYP2C19* genotype, **1*, **2*, and **3* alleles were found in 52.2, 32.6, and 15.2% in the graft liver and 53.9, 35.4, and 10.7% in the native intestine, respectively. The EMs (**1/*1*), IMs (**1/*2* and **1/*3*), and PMs (**2/*2*, **2/*3*, and **3/*3*) of CYP2C19 then were found in 28.1% ($n = 25$), 48.3% ($n = 43$), and 23.6% ($n = 21$) in the graft liver and 30.3% ($n = 27$), 47.2% ($n = 42$), and 22.5% ($n = 20$) in the native intestine, respectively. For the *CYP3A5* genotype, **1* and **3* alleles were found in 19.1 and 80.9% in the graft liver and 20.8 and 79.2% in the native intestine, respectively. Then, the frequencies of *CYP3A5*1* carriers (**1/*1* and **1/*3*) and *CYP3A5*1* noncarriers (**3/*3*) were 33.7% ($n = 30$) and 66.3% ($n = 59$) in the graft liver and 32.6% ($n = 29$) and 67.4% ($n = 60$) in the native intestine, respectively.

To investigate whether intestinal *CYP2C19* polymorphisms affected the interaction between tacrolimus and PPIs, patients were divided based on the *CYP2C19* genotype of transplant recipients (Table 2). The C/D ratio of tacrolimus coadministered with omeprazole was significantly higher in patients with two variant alleles for intestinal *CYP2C19* than those with the wild-type homozygote (*CYP2C19*1/*1*) or heterozygote (*CYP2C19*1/*2* or *CYP2C19*1/*3*) ($P = 0.010$). Likewise, patients with an engrafted liver carrying two variant alleles for *CYP2C19* showed significantly higher C/D ratio than the other groups ($P = 0.022$). Furthermore, the distribution of *CYP3A5*1* noncarriers did not vary between the different *CYP2C19* genotype groups (Table 2). In contrast, the C/D ratio of tacrolimus coadministered with lansoprazole was not associated with *CYP2C19* polymorphisms in the native intestine ($P = 0.52$) or the graft liver ($P = 0.82$).

The tacrolimus C/D ratio between CYP2C19 EMs and IMs was found comparable (Table 2), so that the analyses were carried out between the EMs/IMs versus PMs. In patients receiving omeprazole, the C/D ratio of tacrolimus was significantly increased in PMs compared with EMs/IMs ($P = 0.005$ for native intestine, $P = 0.018$ for graft liver).

Effects of Intestinal and Graft Liver *CYP3A5* Genotypes on the Interaction between Tacrolimus and PPIs. Because we have reported that the *CYP3A5* genotypes of both recipients and donors are important for the oral clearance of tacrolimus in liver transplant recipients (Goto et al., 2004; Fukudo et al., 2006, 2008; Uesugi et al., 2006; Hosohata et al., 2008), we examined the effects of CYP3A5 on the interaction between tacrolimus and PPIs (Table 3). In patients receiving omeprazole, the C/D ratio of tacrolimus was significantly higher in patients with an engrafted liver carrying the *CYP3A5*3/*3* genotype (**1* noncarriers) than the other group (**1* carriers) ($P = 0.034$). Similar trends were observed, although not statistically significant, for the intestinal *CYP3A5* genotype ($P = 0.47$). In patients receiving lansoprazole, **1* noncarriers conferred significantly higher C/D ratio of tacrolimus than **1* carriers ($P = 0.015$ for native intestine, $P = 0.049$ for graft liver).

Effects of the Combination of Intestinal and Graft Liver Genotypes on the Interaction between Tacrolimus and PPIs. As a feature of liver transplantation, the genotypes of recipients (native intestine) are different from those of donors (graft liver) in many cases. Focusing on this feature, we assessed the effects of the combination of intestinal and graft liver *CYP2C19* genotypes on the interaction between tacrolimus and PPIs.

As shown in Fig. 1A, carriers of at least one *CYP2C19* wild-type allele in both the native intestine and the graft liver (EMs/IMs for native intestine and graft liver) showed the lowest values for the tacrolimus C/D ratio (reference group). Compared with the reference group, carriers of at least one *CYP2C19* wild-type allele either in the native intestine or in the graft liver showed almost the same values for the C/D ratio of tacrolimus. However, two *CYP2C19* variant alleles both in the native intestine and in the graft liver (PMs for native intestine and graft liver) conferred a significantly higher (6.9-fold) C/D ratio of tacrolimus than the other groups ($P = 0.0032$). Furthermore, within *CYP3A5*1* noncarriers both in the native intestine and in the graft liver (closed circles, $n = 18$), the C/D ratio was significantly higher in those who also carried two *CYP2C19* variant alleles than any other group ($P = 0.017$), whereas there was no difference among the genotypes carrying at least one *CYP2C19* wild-type allele either in the native intestine or in the graft liver. Conversely, the combination of intestinal and graft liver *CYP2C19* genotypes little affected the C/D ratio of tacrolimus in patients receiving lansoprazole (Fig. 1B).

Experiments in Vitro. Next, we examined the inhibitory effects of PPIs on the metabolism of tacrolimus by CYP3A4 and CYP3A5 using recombinant microsomal preparations. Figure 2 shows representative data among three separate experiments. The apparent inhibition constant (IC_{50}) values (mean ± S.D.) for omeprazole and lansoprazole were 51.9 ± 15.9 and 44.5 ± 18.0 μM for CYP3A4 and 53.7 ± 6.1 and 19.9 ± 13.8 μM for CYP3A5, respectively ($P > 0.05$, omeprazole versus lansoprazole for CYP3A4 and CYP3A5).

TABLE 3

Effects of intestinal and graft liver CYP3A5 genotypes on the C/D ratio of tacrolimus coadministered with omeprazole (n = 35) or lansoprazole (n = 54)

Data are expressed as median (range). **1* carriers, *CYP3A5*1/*1* or**1/*3*; **1* noncarriers, *CYP3A5*3/*3*.

PPI	Variables	*CYP3A5* Genotype		*P*
		**1* Carriers	**1* Noncarriers	
Omeprazole	Native intestine			
	n	11	24	
	Tacrolimus C/D ratio	1.96 (1.04–7.10)	2.34 (0.52–22.9)	0.47
	Graft liver			
	n	14	21	
	Tacrolimus C/D ratio	1.93 (0.52–7.10)	2.54* (1.55–22.9)	0.034
Lansoprazole	Native intestine			
	n	18	36	
	Tacrolimus C/D ratio	1.97 (0.98–11.7)	3.85* (0.72–13.4)	0.015
	Graft liver			
	n	16	38	
	Tacrolimus C/D ratio	1.73 (0.72–11.1)	2.85* (0.98–113.4)	0.049

* $P < 0.05$, *1 carriers versus *1 noncarriers (*U* test).

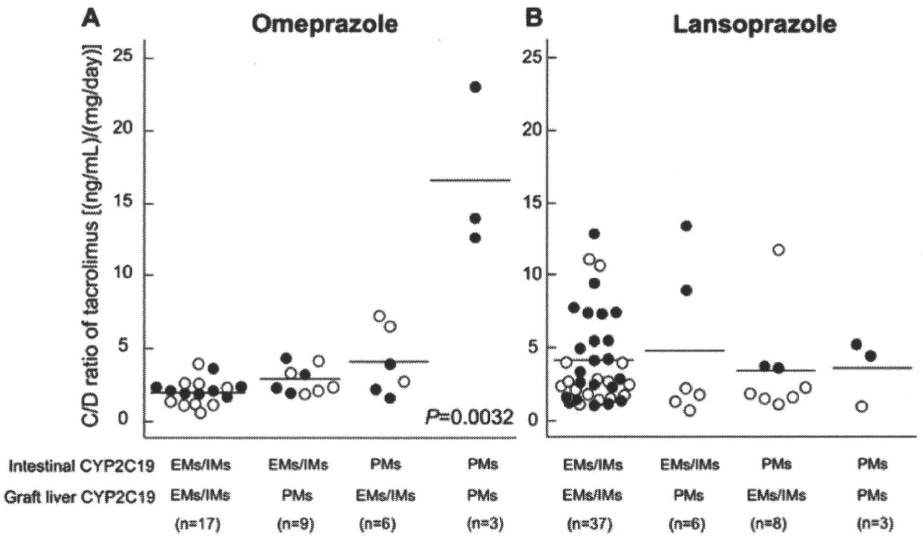

FIG. 1. Effects of the combination of intestinal and graft liver *CYP2C19* genotypes on the C/D ratio of tacrolimus coadministered with omeprazole (A) or lansoprazole (B). Patients were categorized based on the intestinal and graft liver *CYP2C19* genotypes (EMs, *CYP2C19*1/*1*, **1/*2*, and **1/*3*; IMs, *CYP2C19*1/*2* and **1/*3*; PMs, *CYP2C19*2/*2*, **2/*3*, and **3/*3*). The closed circles indicate the *CYP3A5*1* noncarriers (*CYP3A5*3/*3*) both in the native intestine and in the graft liver, and open circles indicate the *CYP3A5*1* carriers (*CYP3A5*1/*1* or **1/*3*). Each bar indicates the median values. *P* values were determined by the Kruskal-Wallis test, followed by the Dunn post hoc test for multiple comparisons.

Discussion

There has been growing recognition that intestinal and hepatic metabolism of orally administered drugs can play a significant role in the first-pass effects (Floren et al., 1997; Hebert, 1997). Despite evaluation of the expressions or catalytic activity of intestinal CYP2C19 (Obach et al., 2001; Lapple et al., 2003; Paine et al., 2006), no studies have assessed the effects of intestinal CYP2C19 on the oral clearance of drugs. The interaction between tacrolimus and PPIs in CYP2C19 PMs are based on indirect effects of PPIs as CYP3A4/5 inhibitors because the main metabolic pathway of PPIs is CYP3A4/5 in CYP2C19 PMs. Furthermore, the direct effects of CYP2C19 on tacrolimus biotransformation can be negligible because tacrolimus never interacts with any P450 drug metabolism enzymes in addition to CYP3A4/5 (Lecointre et al., 2002). Therefore, we focused on the indirect interaction between tacrolimus and PPIs via CYP3A4/5 in patients with the *CYP2C19* polymorphisms, considering the *CYP2C19* genotypes of the native intestine and the graft liver, separately. Our results revealed that LDLT patients with two *CYP2C19* variants in the native intestine and graft liver seemed susceptible to the inhibitory effects of omeprazole, rather than lansoprazole, on the metabolism of tacrolimus (Table 2; Fig. 1). This varying degree of interaction of omeprazole and lansoprazole with tacrolimus in CYP2C19 PMs compared with EMs might be partly because of the different magnitudes of CYP2C19-mediated metabolism among PPIs. The contribution of CYP2C19 in the metabolism of omeprazole is greater than that of lansoprazole (Ishizaki and Horai, 1999). To the best of our knowledge, this is the first study indicating the pharmacokinetic significance of intestinal CYP2C19 in humans in vivo.

In liver transplantation, the genotypes of drug metabolism enzymes between recipients (native intestine) and donors (graft liver) are generally different. Thus, the different genotypes of intestinal and hepatic P450s could regulate the clearance of tacrolimus. In the present study, the C/D ratio of tacrolimus coadministered with omeprazole was significantly high only in cases in which the recipients themselves and their corresponding donors had two variant alleles for *CYP2C19* (Fig. 1A). However, the extent of the increase was attenuated by carrying at least one *CYP2C19* wild-type allele either in the native intestine or in the graft liver, indicating that intestinal and hepatic CYP2C19 could compensate for the functional loss caused by the *CYP2C19* variants in the interaction between tacrolimus and omeprazole in LDLT patients. Considering the relatively high frequency of CYP2C19 PMs in the Japanese population (approximately 20%) (De Morais et al., 1994a), the interaction between tacrolimus and omeprazole is more relevant in Japanese than Caucasian populations. However, this study has clarified that there is a low probability of a strong tacrolimus-omeprazole interaction in liver transplant pa-

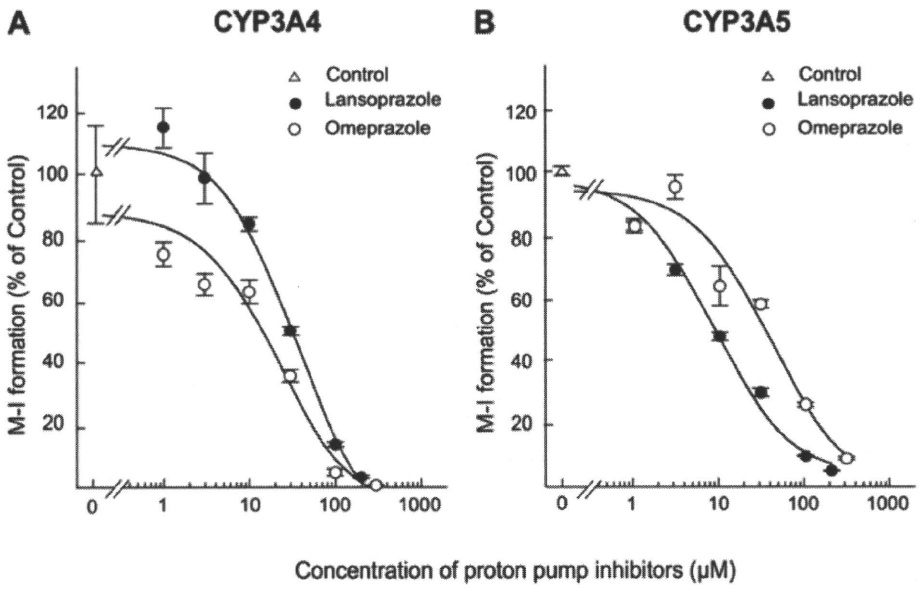

FIG. 2. Concentration-dependent inhibition of the formation of M-I by omeprazole and lansoprazole for CYP3A4 (A) and CYP3A5 (B). Each symbol represents the mean ± S.E. for three independent experiments. The apparent inhibition constant (IC_{50}) values for omeprazole and lansoprazole were 51.9 ± 15.9 and 44.5 ± 18.0 μM for CYP3A4 and 53.7 ± 6.1 and 19.9 ± 13.8 μM for CYP3A5, respectively.

tients because of the extremely small concordance rate of PM genotypes of the recipients with those of their corresponding donors.

We previously reported that intestinal CYP3A5 was significantly associated with the oral clearance of tacrolimus in liver transplant patients (Uesugi et al., 2006). In the present study, CYP3A5 also affected the interaction between tacrolimus and PPIs (Table 3), which is consistent with our experiments in vitro using recombinant microsomes, showing that omeprazole and lansoprazole inhibited the metabolism of tacrolimus via CYP3A4 and CYP3A5 (Fig. 2). Our findings suggest that intestinal and hepatic CYP3A5 is responsible for the interaction between tacrolimus and PPIs. However, even if patients had the *CYP3A5*3/*3* genotype both in the native intestine and in the graft liver (Fig. 1A, closed circles), the C/D ratio of tacrolimus coadministered with omeprazole showed low values when carrying at least one *CYP2C19* wild-type allele either in the native intestine or in the graft liver. These results suggest that the CYP2C19 has a greater effect on overall metabolism of omeprazole than that of CYP3A5. Therefore, in patients receiving omeprazole, carriers of two *CYP2C19* variant alleles both in the native intestine and in the graft liver (PMs/PMs) showed the greatest increased C/D ratio of tacrolimus, and the variability in the metabolism of omeprazole caused by *CYP2C19* polymorphisms is more likely to mask the effects of the *CYP3A5* genotype on the metabolism of tacrolimus. Conversely, in patients receiving lansoprazole, there was no significant difference among the *CYP2C19* genotypes (Table 2), but the *CYP3A5*1* noncarriers conferred a higher tacrolimus C/D ratio than *CYP3A5*1* carriers (Table 3). Our experiments in vitro showed that lansoprazole had a stronger inhibitory effect on the CYP3A5-mediated metabolism of tacrolimus than omeprazole, although not significantly (IC_{50} = 19.9 ± 13.8 μM for lansoprazole, 53.7 ± 6.1 μM for omeprazole) (Fig. 2). The present results are in good agreement with the previous reports that the relative contribution of CYP2C19 against CYP3A4/5 in omeprazole is greater than that in lansoprazole (Ishizaki and Horai, 1999). In addition, our data are also consistent with lansoprazole being a poorer inhibitor of CYP3A4, as suggested by Li et al. (2004).

The present study must be interpreted within the context of its potential limitations. First, we did not have a control group (patients treated with tacrolimus not receiving PPIs). Second, medications including inducers or inhibitors of CYP3A4 were not strictly controlled in both transplant patients and their corresponding donors.

In conclusion, we first showed that the *CYP2C19* defective genotype in the native intestine affected the interaction between tacrolimus and omeprazole in LDLT patients, but the effect was attenuated by the wild-type genotype in the graft liver even when patients had the *CYP3A5*3/*3* genotype in both the native intestine and the graft liver. On the other hand, CYP3A5 rather than CYP2C19 was associated with the interaction between tacrolimus and lansoprazole in liver transplantation. The present findings suggest that the genotyping of *CYP2C19* and *CYP3A5* both in the native intestine and in the graft liver might contribute to safer dosing and monitoring of tacrolimus coadministered with omeprazole and lansoprazole early on after liver transplantation.

References

Andersson T (1996) Pharmacokinetics, metabolism and interactions of acid pump inhibitors. Focus on omeprazole, lansoprazole and pantoprazole. *Clin Pharmacokinet* **31:**9–28.

Christians U, Jacobsen W, Benet LZ, and Lampen A (2002) Mechanisms of clinically relevant drug interactions associated with tacrolimus. *Clin Pharmacokinet* **41:**813–851.

Dai Y, Hebert MF, Isoherranen N, Davis CL, Marsh C, Shen DD, and Thummel KE (2006) Effect of CYP3A5 polymorphism on tacrolimus metabolic clearance in vitro. *Drug Metab Dispos* **34:**836–847.

De Morais SM, Wilkinson GR, Blaisdell J, Meyer UA, Nakamura K, and Goldstein JA (1994a) Identification of a new genetic defect responsible for the polymorphism of (S)-mephenytoin metabolism in Japanese. *Mol Pharmacol* **46:**594–598.

De Morais SM, Wilkinson GR, Blaisdell J, Nakamura K, Meyer UA, and Goldstein JA (1994b) The major genetic defect responsible for the polymorphism of S-mephenytoin metabolism in humans. *J Biol Chem* **269:**15419–15422.

Floren LC, Bekersky I, Benet LZ, Mekki Q, Dressler D, Lee JW, Roberts JP, and Hebert MF (1997) Tacrolimus oral bioavailability doubles with coadministration of ketoconazole. *Clin Pharmacol Ther* **62:**41–49.

Fukudo M, Yano I, Masuda S, Goto M, Uesugi M, Katsura T, Ogura Y, Oike F, Takada Y, Egawa H, et al. (2006) Population pharmacokinetic and pharmacogenomic analysis of tacrolimus in pediatric living-donor liver transplant recipients. *Clin Pharmacol Ther* **80:**331–345.

Fukudo M, Yano I, Yoshimura A, Masuda S, Uesugi M, Hosohata K, Katsura T, Ogura Y, Oike F, Takada Y, et al. (2008) Impact of MDR1 and CYP3A5 on the oral clearance of tacrolimus and tacrolimus-related renal dysfunction in adult living-donor liver transplant patients. *Pharmacogenet Genomics* **18:**413–423.

Goto M, Masuda S, Kiuchi T, Ogura Y, Oike F, Okuda M, Tanaka K, and Inui K (2004) CYP3A5*1-carrying graft liver reduces the concentration/oral dose ratio of tacrolimus in recipients of living-donor liver transplantation. *Pharmacogenetics* **14:**471–478.

Haufroid V, Mourad M, Van Kerckhove V, Wawrzyniak J, De Meyer M, Eddour DC, Malaise J, Lison D, Squifflet JP, and Wallemacq P (2004) The effect of CYP3A5 and MDR1 (ABCB1) polymorphisms on cyclosporine and tacrolimus dose requirements and trough blood levels in stable renal transplant patients. *Pharmacogenetics* **14:**147–154.

Haufroid V, Wallemacq P, VanKerckhove V, Elens L, De Meyer M, Eddour DC, Malaise J, Lison D, and Mourad M (2006) CYP3A5 and ABCB1 polymorphisms and tacrolimus pharmacokinetics in renal transplant candidates: guidelines from an experimental study. *Am J Transplant* **6:**2706–2713.

Hebert MF (1997) Contributions of hepatic and intestinal metabolism and P-glycoprotein to cyclosporine and tacrolimus oral drug delivery. *Adv Drug Deliv Rev* **27:**201–214.

Hesselink DA, van Schaik RH, van der Heiden IP, van der Werf M, Gregoor PJ, Lindemans J, Weimar W, and van Gelder T (2003) Genetic polymorphisms of the CYP3A4, CYP3A5, and

MDR-1 genes and pharmacokinetics of the calcineurin inhibitors cyclosporine and tacrolimus. *Clin Pharmacol Ther* **74:**245–254.
Hosohata K, Masuda S, Ogura Y, Oike F, Takada Y, Katsura T, Uemoto S, and Inui K (2008) Interaction between tacrolimus and lansoprazole, but not rabeprazole in living-donor liver transplant patients with defects of CYP2C19 and CYP3A5. *Drug Metab Pharmacokinet* **23:**134–138.
Inomata Y, Tanaka K, Egawa H, Uemoto S, Ozaki N, Okajima H, Satomura K, Kiuchi T, Yamaoka Y, and Hashida T (1996) The evolution of immunosuppression with FK506 in pediatric living-related liver transplantation. *Transplantation* **61:**247–252.
Ishizaki T and Horai Y (1999) Review article: cytochrome P450 and the metabolism of proton pump inhibitors–emphasis on rabeprazole. *Aliment Pharmacol Ther* **13 (Suppl 3):**27–36.
Itagaki F, Homma M, Yuzawa K, Nishimura M, Naito S, Ueda N, Ohkohchi N, and Kohda Y (2004) Effect of lansoprazole and rabeprazole on tacrolimus pharmacokinetics in healthy volunteers with CYP2C19 mutations. *J Pharm Pharmacol* **56:**1055–1059.
Kahan BD, Keown P, Levy GA, and Johnston A (2002) Therapeutic drug monitoring of immunosuppressant drugs in clinical practice. *Clin Ther* **24:**330–350; discussion 329.
Kamdem LK, Streit F, Zanger UM, Brockmoller J, Oellerich M, Armstrong VW, and Wojnowski L (2005) Contribution of CYP3A5 to the in vitro hepatic clearance of tacrolimus. *Clin Chem* **51:**1374–1381.
Kuypers DR, de Jonge H, Naesens M, Lerut E, Verbeke K, and Vanrenterghem Y (2007) CYP3A5 and CYP3A4 but not MDR1 single-nucleotide polymorphisms determine long-term tacrolimus disposition and drug-related nephrotoxicity in renal recipients. *Clin Pharmacol Ther* **82:**711–725.
Lampen A, Christians U, Guengerich FP, Watkins PB, Kolars JC, Bader A, Gonschior AK, Dralle H, Hackbarth I, and Sewing KF (1995) Metabolism of the immunosuppressant tacrolimus in the small intestine: cytochrome P450, drug interactions, and interindividual variability. *Drug Metab Dispos* **23:**1315–1324.
Lapple F, von Richter O, Fromm MF, Richter T, Thon KP, Wisser H, Griese EU, Eichelbaum M, and Kivisto KT (2003) Differential expression and function of CYP2C isoforms in human intestine and liver. *Pharmacogenetics* **13:**565–575.
Lecointre K, Furlan V, and Taburet AM (2002) In vitro effects of tacrolimus on human cytochrome P450. *Fundam Clin Pharmacol* **16:**455–460.
Li XQ, Andersson TB, Ahlstrom M, and Weidolf L (2004) Comparison of inhibitory effects of the proton pump-inhibiting drugs omeprazole, esomeprazole, lansoprazole, pantoprazole, and rabeprazole on human cytochrome P450 activities. *Drug Metab Dispos* **32:**821–827.
Macphee IA, Fredericks S, Mohamed M, Moreton M, Carter ND, Johnston A, Goldberg L, and Holt DW (2005) Tacrolimus pharmacogenetics: the CYP3A5*1 allele predicts low dose-normalized tacrolimus blood concentrations in whites and South Asians. *Transplantation* **79:**499–502.
Masuda S, Goto M, Fukatsu S, Uesugi M, Ogura Y, Oike F, Kiuchi T, Takada Y, Tanaka K, and Inui K (2006) Intestinal MDR1/ABCB1 level at surgery as a risk factor of acute cellular rejection in living-donor liver transplant patients. *Clin Pharmacol Ther* **79:**90–102.
Masuda S and Inui K (2006) An up-date review on individualized dosage adjustment of calcineurin inhibitors in organ transplant patients. *Pharmacol Ther* **112:**184–198.
Masuda S, Uemoto S, Goto M, Fujimoto Y, Tanaka K, and Inui K (2004) Tacrolimus therapy according to mucosal MDR1 levels in small-bowel transplant recipients. *Clin Pharmacol Ther* **75:**352–361.
Miura M, Inoue K, Kagaya H, Satoh S, Tada H, Sagae Y, Habuchi T, and Suzuki T (2007) Influence of rabeprazole and lansoprazole on the pharmacokinetics of tacrolimus in relation to CYP2C19, CYP3A5 and MDR1 polymorphisms in renal transplant recipients. *Biopharm Drug Dispos* **28:**167–175.
Obach RS, Zhang QY, Dunbar D, and Kaminsky LS (2001) Metabolic characterization of the major human small intestinal cytochrome P450s. *Drug Metab Dispos* **29:**347–352.
Paine MF, Hart HL, Ludington SS, Haining RL, Rettie AE, and Zeldin DC (2006) The human intestinal cytochrome P450 "pie." *Drug Metab Dispos* **34:**880–886.
Shimomura M, Masuda S, Goto M, Katsura T, Kiuchi T, Ogura Y, Oike F, Takada Y, Uemoto S, and Inui K (2008) Required transient dose escalation of tacrolimus in living-donor liver transplant recipients with high concentrations of a minor metabolite M-II in bile. *Drug Metab Pharmacokinet* **23:**313–317.
Shiraga T, Matsuda H, Nagase K, Iwasaki K, Noda K, Yamazaki H, Shimada T, and Funae Y (1994) Metabolism of FK506, a potent immunosuppressive agent, by cytochrome P450 3A enzymes in rat, dog and human liver microsomes. *Biochem Pharmacol* **47:**727–735.
Uesugi M, Masuda S, Katsura T, Oike F, Takada Y, and Inui K (2006) Effect of intestinal CYP3A5 on postoperative tacrolimus trough levels in living-donor liver transplant recipients. *Pharmacogenet Genomics* **16:**119–127.
Venkataramanan R, Swaminathan A, Prasad T, Jain A, Zuckerman S, Warty V, McMichael J, Lever J, Burckart G, and Starzl T (1995) Clinical pharmacokinetics of tacrolimus. *Clin Pharmacokinet* **29:**404–430.
Wang J, Zeevi A, McCurry K, Schuetz E, Zheng H, Iacono A, McDade K, Zaldonis D, Webber S, Watanabe RM, et al. (2006) Impact of ABCB1 (MDR1) haplotypes on tacrolimus dosing in adult lung transplant patients who are CYP3A5 *3/*3 nonexpressors. *Transpl Immunol* **15:**235–240.
Wilkinson GR (2005) Drug metabolism and variability among patients in drug response. *N Engl J Med* **352:**2211–2221.
Yasuhara M, Hashida T, Toraguchi M, Hashimoto Y, Kimura M, Inui K, Hori R, Inomata Y, Tanaka K, and Yamaoka Y (1995) Pharmacokinetics and pharmacodynamics of FK 506 in pediatric patients receiving living-related donor liver transplantations. *Transplant Proc* **27:**1108–1110.
Zheng H, Webber S, Zeevi A, Schuetz E, Zhang J, Bowman P, Boyle G, Law Y, Miller S, Lamba J, et al. (2003) Tacrolimus dosing in pediatric heart transplant patients is related to CYP3A5 and MDR1 gene polymorphisms. *Am J Transplant* **3:**477–483.

Address correspondence to: Ken-ichi Inui, Department of Pharmacy, Kyoto University Hospital, Sakyo-ku, Kyoto 606-8507, Japan. E-mail: inui@kuhp.kyoto-u.ac.jp

A Retrospective Analysis of Vancomycin Pharmacokinetics in Japanese Cancer and Non-cancer Patients Based on Routine Trough Monitoring Data

Shinobu OMOTE,[a,b] Yoshitaka YANO,[c] Tohru HASHIDA,[a] Satohiro MASUDA,[a] Ikuko YANO,[a] Toshiya KATSURA,[a] and Ken-ichi INUI*,[a]

[a] *Department of Pharmacy, Kyoto University Hospital, Faculty of Medicine, Kyoto University; 54 Kawahara-cho, Shogoin, Sakyo-ku, Kyoto 606–8507, Japan:* [b] *Department of Pharmacy, Mitsubishi Kyoto Hospital; 1 Gosyo-cho, Katsura, Nishikyo-ku, Kyoto 615–8087, Japan: and* [c] *Department of Integrative Clinical Pharmacy, Center for Integrative Education of Pharmacy Frontier, Graduate School of Pharmaceutical Sciences, Kyoto University; 46–29 Shimoadachi-cho, Yoshida, Sakyo-ku, Kyoto 606–8501, Japan.*

Received June 13, 2008; accepted October 24, 2008; published online October 28, 2008

The pharmacokinetics of vancomycin was retrospectively examined based on trough concentrations obtained during routine therapeutic drug monitoring to examine possible pharmacokinetic differences between adult Japanese cancer and non-cancer patients with various degrees of renal function. A total of 231 data points from 65 cancer patients and 41 non-cancer patients were collected, and patients' background, vancomycin dose, and vancomycin clearance estimated by an empirical Bayesian method were summarized. Regarding the patients' characteristics and clinical laboratory test data, no clear differences were found between the two groups. The relationship between vancomycin clearance and creatinine clearance were similar between the groups, suggesting little effect of malignancy on vancomycin clearance. After the sub-group comparisons regarding fluid retention and cancer type, no clear differences were found in the vancomycin clearance *versus* creatinine clearance relationship. We conclude that the initial dose of vancomycin should not necessarily be adjusted for cancer patients. For individualized vancomycin-based therapy, dose adjustment at the appropriate time is important according to information from routine therapeutic drug monitoring and clinical laboratory tests, and to observations of the efficacy, nephrotoxicity, and other conditions in each patient.

Key words vancomycin; pharmacokinetics; cancer patient; therapeutic drug monitoring; malignant; methicillin-resistant *Staphylococcus aureus*

Methicillin-resistant *Staphylococcus aureus* (MRSA) is known to cause diseases especially in individuals with less resistance to infectious bacteria, such as elderly, immunosuppressive, or postoperative patients, or patients with total parenteral nutrition (TPN), with trachea catheter or any passage in the trachea, premature infants and newborns, and wound patients. In cancer patients, the risk rate for MRSA infection is generally high because of depressed immunocompetence, a side effect of anticancer agents, and nosocomial infections by MRSA have been reported.[1)]

Vancomycin, a glycopeptide antibiotic, has been used to treat MRSA infections, and it requires effective therapeutic drug monitoring (TDM) during treatment period especially to reduce the incidences of nephrotoxicity by controlling its serum concentration within the therapeutic range.[2—4)] The pharmacokinetics of vancomycin in MRSA-infected patients has been studied,[5—10)] and population pharmacokinetic parameters were reported in adult Japanese patients.[11)] More recently, an empirical Bayesian method has been widely applied to TDM data,[12)] and the predictability of the Bayesian forecasting methodology for vancomycin with the population pharmacokinetic parameters in Japanese patients was examined.[13,14)]

Vancomycin is mainly eliminated into urine, and most of the pharmacokinetic variability can be explained by the degree of renal function.[15)] However, there have been several reports of a difference in vancomycin pharmacokinetics between malignant and non-malignant adult[7,10)] and pediatric[16—18)] patients, suggesting malignant state to be a covariate of the pharmacokinetic variability. Le Normand *et al.*[7)] reported a larger distribution volume and shorter elimination half-life in neutropenic adult patients and they suggested the need of new therapeutic regimen. Fernández de Gatta *et al.*[10)] reported a significant effect of malignancy on clearance in patients with hematologic malignancies and proposed a nomogram for dose setting in cancer patients. Teramachi *et al.*[19)] reported that the clearance was significantly greater in the malignancy group (0.077±0.029 l/h/kg) than non-malignancy group (0.056±0.018 l/h/kg) in Japanese patients. They also found a significant difference in distribution volume at steady state (1.29±0.41 l/kg in malignancy group, 1.05±0.34 l/kg in non-malignancy group). However, it is also true that in their report many patients in the malignancy group showed similar values of clearance and distribution volume to those in the non-malignancy group. Based on these findings, it seems that the strategy for dose setting in cancer patients seems confusing for vancomycin, and even if the mean differences in the pharmacokinetic parameters exist, we considered that dosage individualization based on observed drug concentration data should be much more important as Fernández de Gatta *et al.*[10)] commented, because the inter-individual variability of vancomycin pharmacokinetics is still extensive. Thus in this report, we aimed to clarify the possible impact of such pharmacokinetic differences on the routine vancomycin therapy and performed a retrospective study regarding the pharmacokinetics of vancomycin based on clinical data which were taken in the routine therapeutic drug monitoring in Kyoto University Hospital.

* To whom correspondence should be addressed. e-mail: inui@kuhp.kyoto-u.ac.jp

MATERIALS AND METHODS

Data Source and Patients Characteristics The data from patients treated with vancomycin and monitored as to its serum concentration during hospitalization in Kyoto University Hospital (Kyoto, Japan) were collected retrospectively. The investigation period was from November 2005 to September 2006. Patients under 14 years old or patients with hemodialysis were excluded. The total number of patients was 106, including 65 cancer patients and 41 non-cancer patients. This study was conducted in accordance with the Declaration of Helsinki and its amendments, and the protocol was approved by the Ethics Committee of Kyoto University Graduate School and Faculty of Medicine.

All data were retrospectively collected from the electronic charts, and patient characteristics and results of clinical laboratory tests such as serum creatinine (Scr), blood urea nitrogen (BUN), aspartate aminotransferase (AST), alanine aminotransferase (ALT), and serum albumin (ALB) levels were summarized. Main diagnosis, vancomycin dose, dosing interval, and trough concentration data at steady state were also collected. Serum concentrations were measured by fluorescence polarization immunoassay (FPIA) using a TDxFLx® analyzer (Abbott Japan, Tokyo, Japan) in the Department of Pharmacy, Kyoto University Hospital. Only the trough data at more than 3 d after the initiation of vancomycin therapy were used for the data at steady state. In addition, a steady state condition was confirmed for each patient by visually checking the simulated concentration–time profiles by the Bayesian method described below. In some patients, more than two data points were obtained on different dosing days, and finally, the number of trough concentration values was 145 in cancer patients and 86 in non-cancer patients. In some patients, doses were also changed during treatment, and so we picked the dose and concentration data at typical sampling times, *i.e.* the sampling time when the steady state trough concentration was first measured (referred to as the 'first sampling point') and the sampling time when the concentration data were last measured ('last sampling point'). For daily dose and trough concentration, data were summarized at each of these sampling points. For clinical laboratory tests, values at only the last sampling point were used for further comparison.

Data Analysis The relationships of the observed trough concentration with dose, values of clinical laboratory tests, and patients' other characteristics were examined, and statistical comparisons between the cancer and non-cancer patients were performed accordingly for these observed values. Especially for relationships of the trough concentrations with daily dose, dosing interval, calculated creatinine clearance (CLcr) by the Cockcroft–Gault method,[20] and ALT and ALB were examined by multiple linear regression analysis.

Using the observed trough concentration data, an empirical Bayesian method[21] was applied to obtain the individual estimates of vancomycin clearance (CL). In this study, we obtained the Bayesian estimates for distribution volume but we did not use them for further discussion because only the trough concentration data were available for most patients. Bayesian estimation was carried out using the software package VCM-TDM (Ver. 2.03, Shionogi & Co., Ltd., Osaka, Japan)[22] based on a linear two-compartment model. A population pharmacokinetic parameter set for Japanese adult patients[11] was adopted, where calculated creatinine clearance (CLcr) by the Cockcroft–Gault method[20] was used. That is, in case the calculated CLcr is greater than 85 ml/min, the population average clearance was set to 3.51 l/h, otherwise an equation CL (l/h)=0.0478×CLcr (ml/min) was adopted. All the available trough concentration data in each patient were simultaneously used for the Bayesian estimation. In the patients whose Scr changed more than 0.5 mg/dl, the Bayesian estimates obtained from only the data before the Scr change were used for the following evaluation.

Bayesian predictability was evaluated by a correlation analysis of the observed and predicted values of vancomycin concentration, and mean prediction error (ME) and root mean squared error (RMSE) were used as indices of bias and prediction, respectively[23];

$$\mathrm{ME} = \frac{1}{n}\sum_{i=1}^{n}(C_{\mathrm{pred}} - C_{\mathrm{obs}}) \tag{1}$$

$$\mathrm{RMSE} = \sqrt{\frac{1}{n}\sum_{i=1}^{n}(C_{\mathrm{pred}} - C_{\mathrm{obs}})^2} \tag{2}$$

In Eqs. 1 and 2, n is number of concentration data, C_{pred} is predicted drug concentration and C_{obs} is observed drug concentration.

The cancer patients were divided into sub-groups according to the presence of fluid retention or cancer type, and comparisons of vancomycin clearance were made based on statistical analyses or visual inspection. Type of fluid retention such as ascites and pleural effusion was diagnosed by physicians based on the imaging test, and edema was also diagnosed by physicians by referencing increase of body weight.

Statistical Analysis Mean difference of the patients' characteristics including the results of clinical laboratory tests, vancomycin dose, observed trough concentration, and estimated clearance were tested between the cancer and non-cancer patients. Statistical comparisons were made for the sub-group data, if appropriate, by Student's t-test or Welch's t-test according to results of an F-test for equal variance, with a 5% level of significance. Statistical tests and regression analyses were carried out with Microsoft Excel® (Microsoft, WA, U.S.A.) or Dr. SPSS (SPSS Japan Inc., Tokyo, Japan).

RESULTS

Comparison of Patients' Characteristics The patients' characteristics are summarized in Table 1. No significant differences were found between the two groups for age, body weight, Scr, BUN, AST, ALT, ALB and CLcr. The cancer type and clinical stage in the cancer patients are summarized in Table 2. Most patients were in stage III or IV.

Comparison of Vancomycin Dose and Observed Trough Concentration A summary of the vancomycin dose and observed trough concentration is given in Table 1. In some patients, doses were changed during the treatment, and thus dose and trough concentration at both the first and the last sampling point as defined in the previous section were compared. In the case of the first sampling point, the

Table 1. Summary of Patients' Characteristics

	Cancer	Non-cancer	
Number of patients	65 (male 43, female 22)	41 (male 24, female 17)	
Age (years old)	57.4±14.4 (24—81)	62.6±15.6 (27—92)	N.S.
Body weight (kg)	52.6±11.3 (35.3—94.8)	53.1±10.5 (31.4—78.7)	N.S.
Scr (mg/dl)	0.8±0.8 (0.3—6.1)	0.8±0.4 (0.3—2.2)	N.S.
BUN (mg/dl)	15.8±12.8 (3—76)	18.3±13.6 (3—55)	N.S.
AST (IU/l)	27.9±21.6 (6—129)	35.0±33.1 (8—182)	N.S.
ALT (IU/l)	34.0±32.2 (3—194)	34.5±41.0 (6—245)	N.S.
ALB (g/dl)	3.1±0.5 (1.8—4.5)	3.2±0.6 (1.8—4.4)	N.S.
CLcr (ml/min/kg)[a]	1.69±0.75 (0.21—3.61)	1.62±0.83 (0.42—3.70)	N.S.
CLcr (ml/min)[a]	88.1±40.3 (8.7—181.2)	86.0±46.5 (17.8—203.8)	N.S.
Number of trough measurements	145	86	
Daily dose (mg/kg)[b]	35.5±11.9 (10.5—78.5)	28.5±8.9 (12.2—46.7)	$p<0.01$
Daily dose (mg/kg)[c]	31.4±12.5 (11.8—78.5)	30.4±11.1 (12.2—53.4)	N.S.
Vancomycin conc. (μg/ml)[b]	11.5±5.4 (2.4—29.7)	10.8±5.2 (2.1—24.2)	N.S.
Vancomycin conc. (μg/ml)[c]	11.5±5.0 (2.1—29.7)	12.8±6.4 (2.1—36.6)	N.S.

Values are the mean±S.D. (minimum—maximum). N.S.: Not significantly different. *a*) Calculated by Cockcroft–Gault formula. *b*) At the first sampling point. *c*) At the last sampling point.

Table 2. Cancer Type and Number of Patients in Each Clinical Stage

Cancer type	Stage				Total
	I	II	III	IV	
Acute myelocytic leukemia		Not defined			9
Lung cancer			5	3	8
Esophageal cancer	1		3	2	6
Bladder cancer	2	1		3	6
Malignant lymphoma	1	1	1	2	5
Lymphocytic leukemia		Not defined			4
Pharyngeal cancer		1	1	1	3
Hepatocellular carcinoma				3	3
Soft tissue tumor		Not defined			3
Cervical cancer	1			1	2
Tongue cancer	1		1		2
Multiple myeloma		1	1		2
Pancreatic cancer			1	1	2
Osteosarcoma		Not defined			2
Testicular cancer			1		1
Duodenal neoplasm				1	1
Gastric cancer				1	1
Gallbladder cancer				1	1
Brain tumor		Not defined			1
Adult T-cell leukemia		Not defined			1
Chronic myelocytic leukemia		Not defined			1
Myelodysplastic syndrome		Not defined			1

Not defined: clinical stage is not defined because of non-solid cancer.

dose was 35.5±11.9 mg/kg (mean±S.D.) and 28.5±8.9 mg/kg in the cancer and non-cancer patients, respectively, which were significantly different ($p<0.01$), but the trough concentration was not significantly different (11.5±5.4 μg/ml in the cancer patients and 10.8±5.2 μg/ml in the non-cancer patients). In the case of the last sampling point, no significant differences were found in dose (31.4±12.5 mg/kg *vs.* 30.4±11.1 mg/kg) or trough concentration (11.5±5.0 μg/ml *vs.* 12.8±6.4 μg/ml).

Figures 1 and 2 show the relationship of trough concentration with daily dose (Fig. 1), CLcr (Fig. 2a), ALT as a marker of hepatic function (Fig. 2b), and ALB (Fig. 2c). Multiple linear regression analysis with a stepwise method showed that the trough concentration depends on daily dose ($p<0.001$) and CLcr ($p<0.001$), and was independent of dosing interval, ALT, ALB and cancer type.

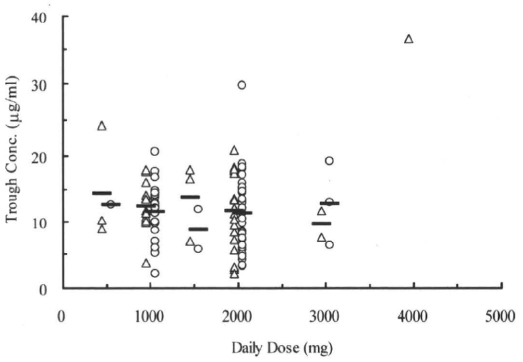

Fig. 1. Relationship of Trough Concentration with Daily Dose

Open circles: cancer patients, open triangles: non-cancer patients. Mean values for each dose are plotted with horizontal bars.

Comparison of Bayesian Estimated Vancomycin Clearance Figure 3 shows a correlation between the observed and the Bayesian predicted vancomycin trough concentrations. The indices ME and RMSE were 0.49 and 2.91, respectively for the cancer patients, and 0.37 and 2.00 for the non-cancer patients. According to these results, Bayesian predictability seems generally acceptable. The accuracy of Bayesian estimation depends on sampling times,[24—26] and it is reported that the estimation error for distribution volume is large but that for clearance is relatively small in case using only trough data.[26] Therefore, we did not compare distribution volume by the Bayesian method between the cancer and non-cancer patients as only trough concentration data were available.

The predicted vancomycin clearance was (mean±S.D., minimum—maximum) 3.73±1.39 (0.912—5.97) l/h for the cancer patients, and 3.48±1.56 (0.545—6.87) l/h for the non-cancer patients, and when adjusted for body weight, clearance was 0.072±0.028 (0.022—0.140) l/h/kg for the cancer patients, and 0.065±0.026 (0.017—0.127) l/h/kg for the non-cancer patients. Although average clearance did not

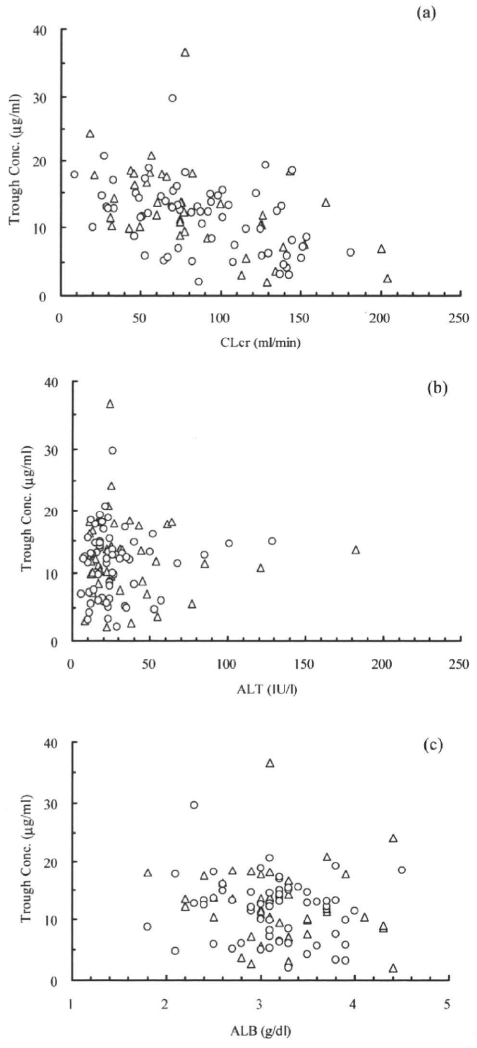

Fig. 2. Relationship of Trough Concentration with (a) Creatinine Clearance (CLcr), (b) Alanine Aminotransferase (ALT), and (c) Serum Albumin (ALB)

Open circles: cancer patients, open triangles: non-cancer patients.

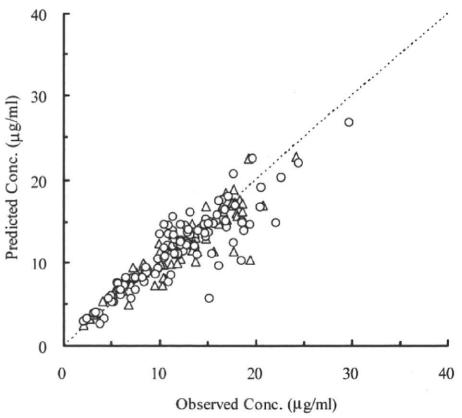

Fig. 3. Correlation Plot for Observed and Predicted Trough Concentrations

Dotted line represents a unit line. Open circles: cancer patients, open triangles: non-cancer patients.

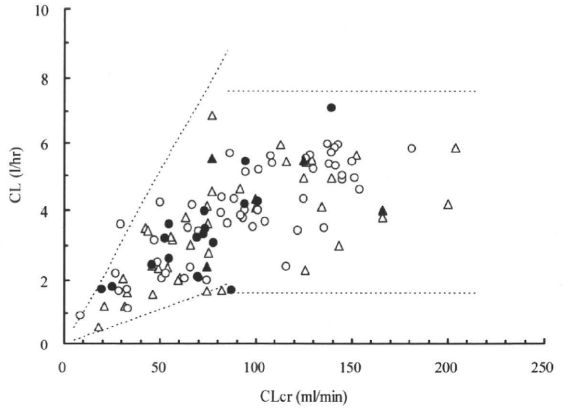

Fig. 4. Correlation of Bayesian Estimated Clearance (CL) and Creatinine Clearance (CLcr)

Circles: data from cancer patients, Triangles: data from non-cancer patients. Data from patients with fluid retention are plotted with closed circles (cancer) or closed triangles (non-cancer). The predictive range given by the mean±2×S.D. of inter-individual variability of the population parameters was given by dotted lines. The lines are discontinuous because the original population profile is discontinuous.

differ significantly between the groups, this does not suggest that there is no effect of malignancy on vancomycin clearance because clearance depends on creatinine clearance, and creatinine clearance varies between patients in the present data set. Therefore visual checking and a comparison of the correlation plots of vancomycin clearance and creatinine clearance in both groups would be a better approach. Figure 4 shows the correlation plots in both groups. The scatters of the data in both groups were similar, suggesting no difference in elimination processes. The similarity of the current data with the previous population data set can be confirmed by comparing the data with a predictive range of CL *vs.* CLcr relationship calculated by 'population mean±2×S.D. of inter-individual variability' as shown in Fig. 4.

Vancomycin distributes abdominal dropsy,[27] and thus we examined the possible difference of vancomycin clearance in patients with fluid retention. A scatter plot of the clearance against creatinine clearance for each sub-group is given in Fig. 4 with closed symbols for those with fluid retention. By visual inspection of Fig. 4, vancomycin clearance in patients with fluid retention was within the range of that in patients without fluid retention.

Estimates of vancomycin clearance were compared among different cancer types. The relationship between clearance (l/h) and creatinine clearance (ml/min) were plotted for each cancer type in Fig. 5. Data for different cancer types with more than 3 patients were plotted separately. Regarding the patients backgrounds, no statistical comparisons were performed because we considered that the numbers of data sets were too small to be used for multiple comparisons, however, mean values for age, body weight, and results of clinical laboratory tests were similar among the cancer types. As shown in Fig. 5, no clear pattern showing the difference by cancer type was found.

DISCUSSION

In this study, the pharmacokinetics of vancomycin was retrospectively examined based on steady state trough concen-

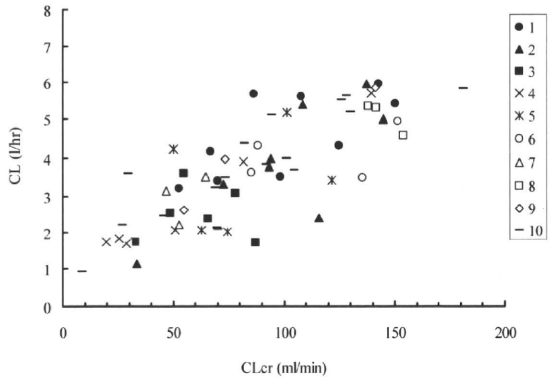

Fig. 5. Correlation of Bayesian Estimated Clearance (CL) and Creatinine Clearance (CLcr) in Patients with Different Cancer Types

Cancer types in the cancer patients are; 1: acute myelocytic leukemia, 2: lung cancer, 3: esophageal cancer, 4: bladder cancer, 5: malignant lymphoma, 6: lymphocytic leukemia, 7: pharyngeal cancer, 8: soft tissue tumor, 9: hepatocellular carcinoma, and 10: others.

trations in routine therapeutic drug monitoring. Although some patients had values outside the recommended concentration range, the trough levels were generally well controlled. As shown in Table 1, average trough concentrations were around 12 μg/ml and were not significantly different between the cancer and non-cancer patients for either the first or last sampling points. Regarding the body weight-normalized dose, the cancer group showed significantly higher values at the first sampling point, however, the doses were not significantly different at the last sampling point. There was one patient with a soft tissue tumor who received a relatively high dose per body weight (38.2 kg body weight, 62 years old, daily dose: 3000 mg/d, 78.5 mg/kg/d). If we exclude this patient, doses did not differ between the two groups. In this patient, body weight was extremely low because of weight loss (15 kg was lost) due to excision of the femoral region and anorexia as a side effect of radiation therapy, and such low body weight resulted in high calculated daily dose per body weight. Based on our present data, vancomycin doses as well as trough concentrations at steady state in routine therapy did not differ between the cancer and non-cancer patients.

From the results of the statistical comparison (Table 1) and visual check of the plot of clearance *versus* creatinine clearance (Fig. 4), there was no clear difference in the estimated clearance between the cancer and non-cancer patients, although there are some reports of a significant pharmacokinetic difference between cancer and non-cancer patients.[7,10,16—18] In the report by Teramachi *et al.*,[19] they selected patients with normal renal function, and they did not have to consider the effect of renal function on their data. In such a well controlled data set, they found some patients that showed greater clearance and distribution volume, however in their report, some individual plots showed similar values of clearance and distribution volume between the malignancy group and non-malignancy group. Based on these findings, we consider that pharmacokinetics of vancomycin may change in some cancer patients but dosage should be individualized based on other covariates such as patients' condition and on observed drug concentration data considering that the inter-individual variability of vancomycin pharmacokinetics is still extensive. In this work, we could not discuss the possible changes in distribution volume because we used only trough concentration data, but as complementary information, we found fluid retention did not affect the vancomycin clearance, and the results suggested no need of dose adjustment for patients with fluid retention to control trough concentration.

Regarding the initial dose adjustment for cancer patients, it is also reported that vancomycin dose should be higher in pediatric cancer patients due to changes of pharmacokinetic parameters.[16—18] However, malignancy state is not the sole covariate affecting vancomycin pharmacokinetics,[10] and also considering a large inter-individual variability in clearance after correcting by each patient's renal function, we should not discuss dosage adjustment in cancer patients based on only average differences between cancer and non-cancer patients. We would suggest that initial dose should not necessarily be increased in cancer patients, but we still should be careful of the possibility that vancomycin concentrations might be lower than expected in cancer patients due to an increase in clearance and/or distribution volume. We consider that peak concentration monitoring is not necessary in routine therapeutic drug monitoring because the side effect can be monitored based on trough levels, and efficacy is related to a ratio of the area under the concentration *vs.* time curve to minimum inhibitory concentration (*AUC*/*MIC*),[6,28] where *AUC* is a function of clearance that can be calculated by the Bayesian method using only trough data.

There are a few reports regarding the effects of cancer type on vancomycin pharmacokinetics in Japanese patients. Teramachi *et al.*[19] reported significant increase in clearance and distribution volume in patients with breast cancer and Hodgkin's lymphoma (n=3 or 4). In our study, we have no data for breast cancer and 5 patients with malignant lymphoma. For the latter, vancomycin dose and clearance showed similar values as shown in Fig. 5 although the numbers of cases are small. In other cancer groups, although it is difficult to compare the pharmacokinetics precisely, by visually checking the plots, no clear dependence on cancer type was found for clearance.

In our present analysis, we found no clear difference in vancomycin clearance between the cancer and non-cancer patients, and therefore we conclude that initial dose should not necessarily be adjusted (increased) for cancer patients. In dosage adjustment in routine therapeutic drug monitoring according to a Bayesian prediction, one trough concentration is usually enough to establish an individualized dosage.[14,29] Of course in all patients, dose adjustment at the appropriate time is important according to information from routine therapeutic drug monitoring and clinical laboratory tests, and should be based also on observations of efficacy, nephrotoxicity and other conditions in each patient.

REFERENCES

1) Sakai C., Satoh Y., Ohkusu K., Kumagai K., Ishii A., *J. Jpn. Assoc. Infect. Dis.*, **75**, 940—945 (2001).
2) Fernández de Gatta M., Calvo M. V., Hernández J. M., Caballero D., San Miguel J. F., Domínguez-Gil A., *Clin. Pharmacol. Ther.*, **60**, 332—340 (1996).
3) MacGowan A. P., *Ther. Drug Monit.*, **20**, 473—477 (1998).
4) Iwamoto T., Kagawa Y., Kojima M., *Biol. Pharm. Bull.*, **26**, 876—879 (2003).
5) Leader W. G., Chandler M. H., *Clin. Pharmacokinet.*, **28**, 327—342

(1995).
6) Rybak M. J., *Clin. Infect. Dis.*, **42**, S35—S39 (2006).
7) Le Normand Y., Milpied N., Kergueris M. F., Harousseau J. L., *Int. J. Biomed. Comput.*, **36**, 121—125 (1994).
8) Buelga D. S., Fernandez de Gatta M., Herrera E. V., Dominguez-Gil A., García M. J., *Antimicrob. Agents Chemother.*, **49**, 4934—4941 (2005).
9) Aldaz A., Ortega A., Idoate A., Giraldez J., Bougarolas A., *Ther. Drug Monit.*, **22**, 250—257 (2000).
10) Fernández de Gatta M., Fruns I., Hernández J. M., Caballero D., San Miguel J. F., Martínez Lanao J., Domínguez-Gil Hurlé A., *Clin. Pharm.*, **12**, 515—520 (1993).
11) Yasuhara M., Iga T., Zenda H., Okumura K., Oguma T., Yano Y., Hori R., *Ther. Drug. Monit.*, **20**, 139—148 (1998).
12) Jelliffe R. W., Schumitzky A., Bayard D., Milman M., Guilder M. V., Wang X., Jiang F., Barbaut X., Maire P., *Clin. Pharmacokinet.*, **34**, 57—77 (1998).
13) Teramachi H., Hatakeyama H., Matsushita R., Imai Y., Miyamoto K., Tsuji A., *Biol. Pharm. Bull.*, **25**, 1333—1338 (2002).
14) Ohnishi A., Yano Y., Shimamura K., Oguma T., *Biol. Pharm. Bull.*, **24**, 1446—1450 (2001).
15) Matzke G. R., "Applied Pharmacokinetics," 2nd ed., ed. by Evans W. E., Schentag J. J., Jusko W. J., Applied Therapeutics, Inc., Spokane, WA, 1986.
16) Chang D., Lime L., Malogolowkin M., *Pediatr. Infect. Dis. J.*, **13**, 969—974 (1994).
17) Krivoy N., Peleg S., Postovsky S., Arush M. W. B., *Pediatr. Hematol. Oncol.*, **15**, 333—338 (1998).
18) Chang D., *Pediatr. Infect. Dis. J.*, **14**, 667—673 (1995).
19) Teramachi H., Matsushita R., Tsuji A., *Jpn. J. Chemother.*, **53**, 357—363 (2005). (in Japanese except Abstract)
20) Cockcroft D. W., Gault M. H., *Nephron*, **16**, 31—41 (1976).
21) Sheiner L. B., Beal S. L., *J. Pharm. Sci.*, **71**, 1344—1348 (1982).
22) Yano Y., Oguma T., *Jpn. J. Ther. Drug Monit.*, **14**, 179—188 (1997). (in Japanese except Abstract).
23) Sheiner L. B., Beal S. L., *J. Pharmacokinet. Biopharm.*, **9**, 503—512 (1981).
24) Tsuchiwata S., Mihara K., Yafune A., Ogata H., *Ther. Drug Monit.*, **27**, 18—24 (2005).
25) Mahmood I., *Int. J. Clin. Pharmacol. Ther.*, **41**, 392—396 (2003).
26) Ohnishi A., Yano Y., Ishibashi T., Katsube T., Oguma T., *Drug Metab. Pharmacokinet.*, **20**, 415—422 (2005).
27) Moellering R. C., Krogstad D. J., Greenblatt D. J., *Rev. Infect. Dis.*, **3S**, S230—S235 (1981).
28) Moise-Broder P. A., Forrest A., Birmingham M. C., Schentag J. J., *Clin. Pharmacokinet.*, **43**, 925—942 (2004).
29) Igarashi M., Nakatani T., Hayashi M., Nakata K., Kasuya Y., *Jpn. J. Chemother.*, **50**, 826—829 (2005). (in Japanese except Abstract)

0022-3565/09/3291-185–191$20.00
THE JOURNAL OF PHARMACOLOGY AND EXPERIMENTAL THERAPEUTICS
JPET 329:185–191, 2009

Vol. 329, No. 1
147918/3454091
Printed in U.S.A.

Involvement of Human Multidrug and Toxin Extrusion 1 in the Drug Interaction between Cimetidine and Metformin in Renal Epithelial Cells

Masahiro Tsuda, Tomohiro Terada, Miki Ueba, Tomoko Sato, Satohiro Masuda, Toshiya Katsura, and Ken-ichi Inui

Department of Pharmacy, Kyoto University Hospital, Faculty of Medicine, Kyoto University, Kyoto, Japan

Received October 24, 2008; accepted January 21, 2009

ABSTRACT

In human proximal tubules, organic cations are taken up from blood into cells by human organic cation transporter 2 [hOCT2/solute carrier (SLC) 22A2] and then eliminated into the lumen by apical H^+/organic cation antiporters, human multidrug and toxin extrusion 1 (hMATE1/SLC47A1) and hMATE2-K (SLC47A2). To evaluate drug interactions of cationic drugs in the secretion process, epithelial cells engineered to express both hOCT2 and hMATE transporters are required to simultaneously evaluate drug interactions with renal basolateral and apical organic cation transporters. In the present study, therefore, we assessed the drug interaction between cimetidine and metformin with double-transfected Madin-Darby canine kidney cells stably expressing both hOCT2 and hMATE1 as an in vitro model of the proximal tubular epithelial cells. The basolateral-to-apical transport and intracellular accumulation of [^{14}C]metformin by a double transfectant were markedly inhibited by 1 mM cimetidine at the basolateral side. On the other hand, 1 μM cimetidine at the basolateral side moderately decreased the basolateral-to-apical transport of [^{14}C]metformin and significantly increased the intracellular accumulation of [^{14}C]metformin from the basolateral side, suggesting that cimetidine at a low concentration inhibits apical hMATE1, rather than basolateral hOCT2. Actually, in concentration-dependent inhibition studies by a single transporter expression system, such as human embryonic kidney 293 stably expressing hMATE1, hMATE2-K, or hOCT2, cimetidine showed higher affinity for hMATEs than for hOCT2. These results suggest that apical hMATE1 is involved in drug interactions between cimetidine and cationic compounds in the proximal tubular epithelial cells.

Drug interactions involving metabolism and/or excretion cause marked changes in plasma and intracellular concentrations of the affected drug. Such interactions can lead to severe adverse effects or unexpected pharmacological effects. Recent studies have shown that many transporters play important roles in the uptake and subsequent secretion of drugs in the liver and kidney, and several specific transporter proteins involved in drug interactions have been reported (Shitara et al., 2005; Endres et al., 2006; Li et al., 2006). However, most of these reports examined the involvement of either apical or basolateral transporters. To reproduce drug interactions via renal transporters in vivo, analyses by the epithelial cells with transcellular transport systems are needed.

This work was supported in part by the Ministry of Health, Labor and Welfare of Japan [Health and Labor Sciences Research Grants]; and the Ministry of Education, Science, Culture and Sports of Japan [Grant-in-aid for Scientific Research].

Article, publication date, and citation information can be found at http://jpet.aspetjournals.org.

doi:10.1124/jpet.108.147918.

In human proximal tubules, organic cations are taken up from blood into cells by human organic cation transporter 2 (hOCT2/SLC22A2) and then eliminated into the lumen by apical H^+/organic cation antiporters, human multidrug and toxin extrusion 1 (hMATE1/SLC47A1) and hMATE2-K (SLC47A2). hMATE1 and hMATE2-K have been identified recently (Otsuka et al., 2005; Masuda et al., 2006), and we have characterized both transporters in terms of tissue distribution, membrane localization, transcriptional regulation, and transport characteristics (Terada and Inui, 2008). However, there has been little systematic comparison of substrate affinity among hMATE1, hMATE2-K, and hOCT2. Comparisons of substrate affinity for hMATEs and hOCT2 would enable us to predict where drug interactions between cationic drugs are likely to occur in the renal secretion process in vivo. It is important to predict where on the membrane drug interaction will occur because the intracellular accumulation of drugs at the proximal tubules may be involved in drug-induced nephrotoxicity.

Here, for a systematic comparison of substrate affinity

ABBREVIATIONS: h, human; OCT, organic cation transporter; SLC, solute carrier; MATE, multidrug and toxin extrusion; MDCK, Madin-Darby canine kidney; TEA, tetraethylammonium; HEK, human embryonic kidney; r, rat.

among hMATE1, hMATE2-K, and hOCT2, the affinity of various drugs for hMATE1 and hMATE2-K was elucidated. Then, based on a comparison of the affinity for the hMATE family and hOCT2, the involvement of hMATE1 in the drug interaction between cimetidine and metformin was evaluated by using double-transfected Madin-Darby canine kidney (MDCK) cells stably expressing both hOCT2 and hMATE1 (MDCK-hOCT2/hMATE1 cells). Recently, we have established this double transfectant, and demonstrated that MDCK-hOCT2/hMATE1 cells are an appropriate in vitro model of human tubular epithelial cells to evaluate the transcellular transport of cationic drugs (Sato et al., 2008).

Materials and Methods

Materials. Pramipexole dihydrochloride monohydrate and talipexole hydrochloride were kindly provided by Nippon Boehringer Ingelheim (Tokyo, Japan). [^{14}C]Tetraethylammonium (TEA) (2.035 GBq/mmol) was purchased from American Radiolabeled Chemicals (St. Louis, MO). [^{14}C]Metformin (962 MBq/mmol) and D-[^{14}C]mannitol (2 GBq/mmol) were purchased from Moravek Biochemicals (Brea, CA). [*N*-Methyl-^{3}H]cimetidine (470 GBq/mmol) was obtained from GE Healthcare (Chalfont St. Giles, UK). D-[1-^{3}H(N)]mannitol (525.4 GBq/mmol) was acquired from PerkinElmer Life and Analytical Sciences (Boston, MA). Quinidine sulfate, verapamil hydrochloride, imipramine hydrochloride, diphenhydramine hydrochloride, (±)-chlorpheniramine maleate, and cimetidine were purchased from Nacalai Tesque (Kyoto, Japan). Metformin hydrochloride, diltiazem hydrochloride, procainamide hydrochloride, ranitidine hydrochloride, and amantadine hydrochloride were obtained from Sigma-Aldrich (St. Louis, MO). Disopyramide, desipramine hydrochloride and famotidine were acquired from Wako Pure Chemicals (Osaka, Japan). Cetirizine was obtained from LKT Labs (St. Paul, MN). All other chemicals used were of the highest purity available.

Cell Culture. According to our previous report (Tanihara et al., 2007), HEK293 cells stably expressing hMATE1 (HEK-hMATE1 cells) or hMATE2-K (HEK-hMATE2-K cells) were cultured in complete medium consisting of Dulbecco's modified Eagle's medium (Sigma-Aldrich) with 10% fetal bovine serum (Invitrogen, Carlsbad, CA) and hygromycin B (0.2 mg/ml; Invitrogen) in an atmosphere of 5% CO_2/95% air at 37°C. The double-transfected MDCK-hOCT2/hMATE1 cells were previously established in our laboratory (Sato et al., 2008). MDCK-hOCT2/hMATE1 cells were cultured in complete medium consisting of Dulbecco's modified Eagle's medium with 10% fetal bovine serum, hygromycin B (0.2 mg/ml), and G-418 (0.5 mg/ml; Nacalai Tesque) in an atmosphere of 5% CO_2/95% air at 37°C. In the previous study, we demonstrated that hOCT2 and hMATE1 were localized on the basolateral and apical membrane, respectively, in MDCK-hOCT2/hMATE1 cells by immunofluorescence microscopy (Sato et al., 2008). HEK293 cells stably expressing hOCT2 (HEK-hOCT2 cells) were cultured according to a previous report (Urakami et al., 2004).

Preparation of Membrane Vesicles from HEK-hMATE1 and HEK-hMATE2-K Cells. HEK-hMATE1 or HEK-hMATE2-K cells were seeded on 100-mm plastic dishes (5×10^6 cells/dish), with 25 dishes used in a single preparation. Then, plasma membrane vesicles were prepared according to our previous report (Tsuda et al., 2007).

Transport Experiments by Membrane Vesicles. The uptake of [^{14}C]TEA by membrane vesicles from HEK-hMATE1 or HEK-hMATE2-K cells was measured using a rapid filtration technique according to our previous report (Tsuda et al., 2007). Nonspecific absorption was determined by the addition of [^{14}C]TEA to 1 ml of ice-cold stop solution containing 20 μl of membrane vesicles. This value was subtracted from the total uptake data. The protein content was determined by the method of Bradford (1976) using a Bio-Rad Protein Assay Kit (Bio-Rad, Hercules, CA) with bovine γ-globulin as a standard.

Transport Experiments by Transfectants. The cellular uptake of radiolabeled compounds was performed as reported previously (Urakami et al., 2004; Tanihara et al., 2007). The transcellular transport experiments with radiolabeled compounds were performed as described previously (Sato et al., 2008). In brief, MDCK-hOCT2/hMATE1 cells were seeded on microporous membrane filters (3.0-μm pores, 4.7-cm^2 growth area) inside a Transwell cell culture chamber (Corning Life Sciences, Lowell, MA) at a density of 18×10^5 cells/well. On the 7th day after the seeding, the cells were used for transcellular transport experiments. The composition of the incubation medium was as follows: 145 mM NaCl, 3 mM KCl, 1 mM $CaCl_2$, 0.5 mM $MgCl_2$, 5 mM D-glucose, and 5 mM HEPES, pH 7.4, or MES, pH 6.0. After the removal of the culture medium from both sides of the monolayers, the cell monolayers were preincubated with 2 ml of incubation medium, pH 7.4, on each side for 10 min at 37°C. Then, 2 ml of incubation medium, pH 7.4, containing both a radiolabeled compound and radiolabeled mannitol was added to the basolateral side, and 2 ml of nonradioactive incubation medium, pH 6.0, was added to the apical side. The monolayers were incubated for specified periods of time at 37°C. Radiolabeled mannitol, a compound that is not transported by the cells, was used to calculate paracellular flux and the extracellular trapping of substrates. For transport measurements, an aliquot (100 μl) of the incubation medium on the apical side was taken at specified times, and the radioactivity was determined in 5 ml of ACSII by liquid scintillation counting. For accumulation studies, the medium was removed by aspiration at the end of the incubation period, and the monolayers were rapidly washed twice with 2 ml of ice-cold incubation medium, pH 7.4, on each side. The filters were detached from the chambers, the cells on the filters were solubilized with 0.5 ml of 0.5 N NaOH, and the radioactivity in aliquots (300 μl) was determined in 3 ml of ACSII by liquid scintillation counting. The protein content of the solubilized cells was determined using a Bio-Rad Protein Assay Kit with bovine γ-globulin as a standard (Bradford, 1976).

Measurement of Intracellular Volume. The equilibrium uptake of sulfanilamide was determined according to standard procedures for transcellular transport experiments with a slight modification. In brief, after the preincubation, 2 ml of incubation medium, pH 7.4, containing both 10 mM sulfanilamide and D-[^{3}H]mannitol was added to both sides. The intracellular volume was calculated from the equilibrium uptake (60 min) and external concentration of sulfanilamide. Sulfanilamide was diazotized and coupled with 2-DEAE-1-naphthylamine oxalate, and the amount of colored material was determined spectrophotometrically at 550 nm (Saito et al., 1986).

Data Analysis. Data were expressed as the means ± S.D. Two or three experiments were conducted, and representative results were shown. Apparent K_i values were expressed as the means ± S.E. and analyzed statistically using the unpaired Student's *t* test. Data from transport experiments were analyzed statistically with the one-way analysis of variance followed by Dunnett's test.

Results

Determination of the Driving Force of hMATE1 and hMATE2-K with Membrane Vesicles from HEK-hMATE1 and HEK-hMATE2-K Cells. At first, to validate the driving force of hMATE1 and hMATE2-K, we carried out [^{14}C]TEA uptake studies with membrane vesicles from HEK-hMATE1 or HEK-hMATE2-K cells. In the presence of an outwardly directed H^+ gradient, a marked stimulation of [^{14}C]TEA uptake (overshoot phenomenon) was observed in membrane vesicles from HEK-hMATE1 and HEK-hMATE2-K cells (Fig. 1, A and B). Furthermore, [^{14}C]TEA uptake by hMATE1 and hMATE2-K was not altered by the presence of valinomycin with or without

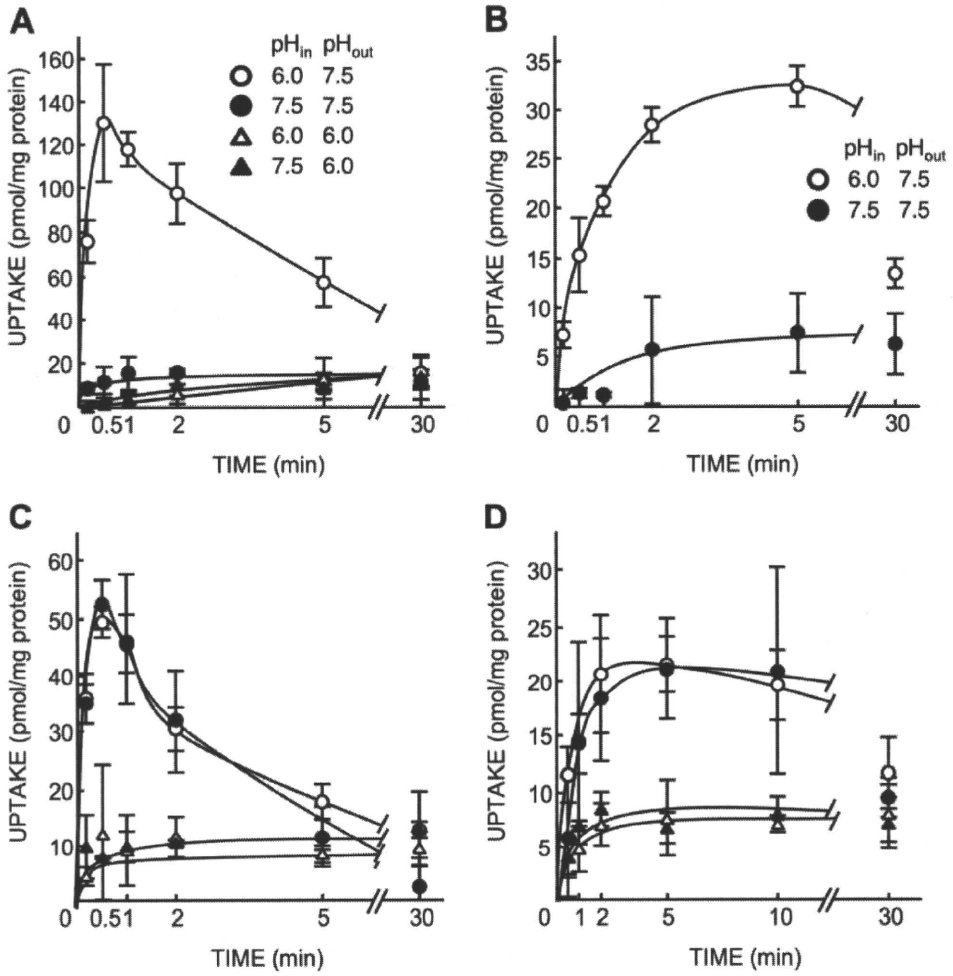

Fig. 1. Determination of the driving force of the hMATE family with membrane vesicles from HEK-hMATE1 (A and C) and HEK-hMATE2-K (B and D) cells. A and B, effects of various H^+ gradients on [^{14}C]TEA uptake. Membrane vesicles were prepared in the experimental buffer at pH 6.0 (○ and △) or 7.5 (● and ▲). The uptake of [^{14}C]TEA was examined in the experimental buffer containing 31.25 μM [^{14}C]TEA and 100 mM KCl at pH 6.0 (△ and ▲) or 7.5 (○ and ●). C and D, effects of valinomycin on [^{14}C]TEA uptake with or without a H^+ gradient. Membrane vesicles were prepared in the experimental buffer at pH 6.0 (○ and ●) or 7.5 (△ and ▲). The uptake of [^{14}C]TEA was examined in the experimental buffer containing 31.25 μM [^{14}C]TEA and 100 mM CsCl at pH 7.5 in the absence (○ and △) or presence (● and ▲) of 8 μM valinomycin. Valinomycin, a K^+ ionophore, was employed to produce an inside-negative membrane potential in the presence of outward K^+ gradient. Each point represents the mean ± S.D. for three determinations. These figures are representative of two separate experiments. pH_{in}, intravesicular pH; pH_{out}, extravesicular pH.

the H^+ gradient (Fig. 1, C and D). These findings indicated that both transporters utilized an oppositely directed H^+ gradient as a driving force. Subsequent experiments were carried out in the presence of an outwardly directed H^+ gradient to evaluate the transport characteristics of the MATE family.

Comparison of Substrate Affinity for hMATE1, hMATE2-K, and hOCT2. To compare the substrate affinity for hMATE1 and hMATE2-K, the apparent K_i values of various cationic drugs for the uptake of [^{14}C]TEA were determined. Cationic drugs inhibited [^{14}C]TEA uptake via hMATE1 and hMATE2-K in a dose-dependent manner. Figures 2 and 3 show representative inhibition curves of histamine H_2 receptor antagonists and antiparkinsonian agents, respectively. Table 1 provides a summary of the apparent K_i values of various drugs for hMATE1 and hMATE2-K. Histamine H_2 receptor antagonists such as cimetidine and famotidine showed high affinity for hMATE1 and hMATE2-K as compared with other drugs. Although many drugs tended to have higher affinity for hMATE1 than for hMATE2-K, only pramipexole, an antiparkinsonian agent, exhibited higher affinity for hMATE2-K than for hMATE1. Table 2 shows the affinity for hMATE1, hMATE2-K, and OCT2 of various compounds excreted from the kidney. K_m values of hOCT2 and rat (r) OCT2 were cited from previous papers (Urakami et al., 2001; Ishiguro et al., 2005; Koepsell et al., 2007). Most drugs showed higher affinity for OCT2 than for hMATEs.

Effects of Cimetidine on Transcellular Transport of [^{14}C]Metformin in MDCK-hOCT2/hMATE1 Cells. It is interesting that histamine H_2 receptor antagonists such as cimetidine showed higher affinity for hMATEs than for hOCT2 (Table 2). Furthermore, recent clinical pharmacokinetic and pharmacogenomic analyses of metformin have paid attention to the renal secretion process (Shikata et al., 2007; Song et al., 2008; Takane et al., 2008; Wang et al., 2008). Therefore, we examined the effect of different concentrations of cimetidine on the basolateral-to-apical transport and intracellular accumulation of [^{14}C]metformin in MDCK-hOCT2/hMATE1 cells. We have demonstrated recently that MDCK-hOCT2/hMATE1 showed the vectorial transcellular transport of organic cations, such as TEA and metformin

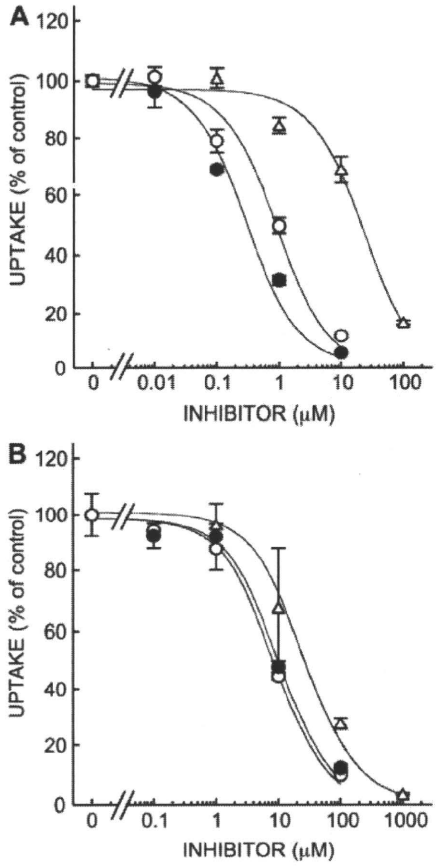

Fig. 2. Effects of histamine H_2 receptor antagonists on [^{14}C]TEA uptake by HEK-hMATE1 (A) and HEK-hMATE2-K (B) cells. HEK-hMATE1 and HEK-hMATE2-K cells were preincubated with 30 mM NH_4Cl, pH 7.4, for 20 min. Then, the preincubation medium was removed, and the cells were incubated with 5 μM [^{14}C]TEA in the presence of cimetidine (○), famotidine (●), or ranitidine (△) for 1 min at 37°C (pH 7.4). After the incubation, the radioactivity of solubilized cells was measured. Each point represents the mean ± S.D. for three monolayers. These figures are representative of three separate experiments.

(Sato et al., 2008). As shown in Fig. 4A, the transcellular transport of [^{14}C]metformin was moderately inhibited by the presence of 1 μM cimetidine and almost completely inhibited by the presence of 1 mM cimetidine. The cellular accumulation of [^{14}C]metformin was inhibited by 1 mM cimetidine but increased by 1 μM cimetidine (Fig. 4B). Furthermore, we examined the inhibitory effects of cimetidine on the uptake of [^{14}C]metformin by hOCT2. Cimetidine had little effect at 1 μM but inhibited the uptake at 1 mM (Fig. 5). The apparent K_i value of cimetidine for hOCT2 was calculated to be 147.1 ± 11.0 μM. These results suggest that 1 mM cimetidine competitively inhibits the uptake of [^{14}C]metformin by hOCT2, resulting in a drastic decrease in both the transcellular transport and the intracellular accumulation of [^{14}C]metformin. On the other hand, 1 μM cimetidine inhibits the apical efflux of [^{14}C]metformin via hMATE1, but not the uptake by hOCT2, causing a marked increase in its cellular accumulation.

Intracellular Concentration of [^{3}H]Cimetidine in MDCK-hOCT2/hMATE1 Cells. To confirm that hMATE1 is specifically inhibited by intracellular cimetidine taken up from the basolateral side, the intracellular concentration of cimetidine was determined. The amount of intracellular cimetidine after 60 min of incubation was demonstrated to be 10.0 ± 0.5 pmol/mg protein. We then measured the intracellular volume of MDCK-hOCT2/hMATE1 cells with the equilibrium uptake of sulfanilamide and found that it was 2.2 ± 0.4 μl/mg protein. Based on these findings, the intracellular concentration of cimetidine was calculated as 4.5 ± 0.4 μM. Considering the K_i values of cimetidine for hMATE1 and hOCT2, this intracellular concentration suggests that the transport of cationic drugs via hMATE1 is specifically inhibited by intracellular cimetidine, but transport via hOCT2 is little inhibited by intracellular cimetidine (Fig. 6).

Discussion

We reported that hMATE1 and hMATE2-K have a similar substrate specificity for many endogenous organic cations and cationic drugs and that several substrates have higher affinity for hMATE1 than for hMATE2-K (Tanihara et al., 2007). In the present study, four cationic drugs had similar affinity for hMATE1 and for hMATE2-K, and 12 cationic drugs were found to have higher affinity for hMATE1 than for hMATE2-K (Table 1). This would suggest that hMATE1 and hMATE2-K have complementary roles in the renal se-

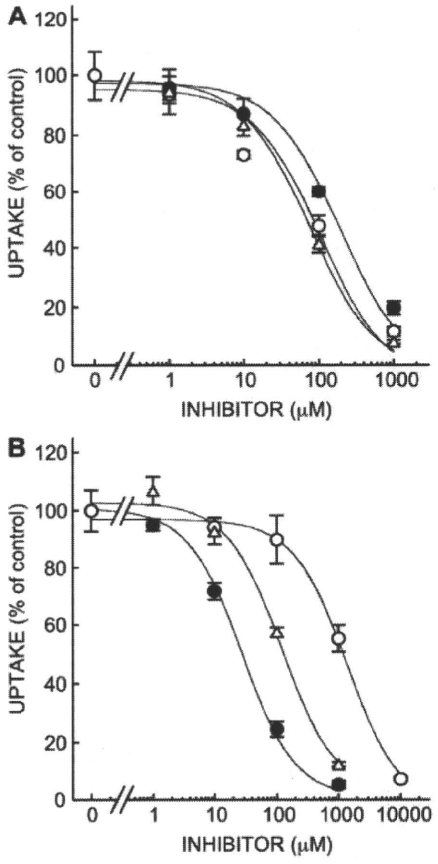

Fig. 3. Effects of antiparkinsonian agents on [^{14}C]TEA uptake by HEK-hMATE1 (A) and HEK-hMATE2-K (B) cells. HEK-hMATE1 and HEK-hMATE2-K cells were preincubated with 30 mM NH_4Cl, pH 7.4, for 20 min. Then, the preincubation medium was removed, and the cells were incubated with 5 μM [^{14}C]TEA in the presence of amantadine (○), pramipexole (●), or talipexole (△) for 1 min at 37°C, pH 7.4. After the incubation, the radioactivity of solubilized cells was measured. Each point represents the mean ± S.D. for three monolayers. These figures are representative of three separate experiments.

TABLE 1
The apparent K_i values of various drugs for [^{14}C]TEA uptake by hMATE1 and hMATE2-K
Each value represents the mean ± S.E. for three independent experiments.

Drug	Apparent K_i Values for [^{14}C]TEA Uptake		Ratio of K_i Values (hMATE1/hMATE2-K)
	hMATE1	hMATE2-K	
	μM		
Antidiabetic drug			
Metformin	666.9 ± 30.2	6515.7 ± 792.4	0.10
Antiarrhythmic drugs			
Diltiazem	12.5 ± 0.7	117.0 ± 2.7*	0.11
Disopyramide	83.8 ± 5.8	291.6 ± 38.3*	0.29
Procainamide	217.0 ± 11.6	178.1 ± 19.3	1.22
Quinidine	29.2 ± 3.1	23.1 ± 4.5	1.26
Verapamil	27.5 ± 3.6	32.1 ± 4.4	0.85
Antidepressant drugs			
Desipramine	55.7 ± 14.5	283.0 ± 53.5*	0.19
Imipramine	42.0 ± 9.0	182.9 ± 31.0*	0.23
Histamine H_1 receptor antagonists			
Cetirizine	371.2 ± 42.7	817.6 ± 103.6*	0.45
Chlorpheniramine	87.6 ± 8.5	191.2 ± 33.6*	0.46
Diphenhydramine	87.0 ± 4.0	266.5 ± 53.4*	0.33
Histamine H_2 receptor antagonists			
Cimetidine	1.1 ± 0.3	7.3 ± 0.7*	0.15
Famotidine	0.6 ± 0.2	9.7 ± 0.4*	0.06
Ranitidine	25.4 ± 2.1	25.0 ± 0.8	1.02
Antiparkinsonian agents			
Amantadine	111.8 ± 5.9	1167.0 ± 100.5*	0.10
Pramipexole	141.4 ± 24.2	24.1 ± 3.4*	5.86
Talipexole	66.0 ± 3.7	119.5 ± 15.3*	0.55

* $P < 0.05$, significantly different from the apparent K_i value of hMATE1.

cretion of organic cations. It is interesting that only pramipexole showed markedly higher affinity for hMATE2-K than for hMATE1 (Fig. 3; Table 1). It has been reported that pramipexole is transported by rOCT1 and rOCT2 (Ishiguro et al., 2005), but it is unclear whether pramipexole is transported by the hMATE family and hOCT2. Pramipexole may be a good probe to distinguish the molecular mechanisms by which the hMATE family recognizes substrates.

In the present study, most drugs showed higher affinity for OCT2 than for hMATEs (Table 2). Histamine H_2 receptor antagonists such as cimetidine and famotidine, however, showed higher affinity for hMATEs than for hOCT2. In particular, the K_i values of cimetidine for hMATE1 and for hOCT2 were 1.1 and 8.6 to 73 μM (Koepsell et al., 2007), respectively. Taking into consideration the effective blood concentration of cimetidine (2.0–3.6 μM) (Benet et al., 1996), it is assumed that hOCT2 is little inhibited by cimetidine at clinical doses, but hMATE1 is inhibited by cimetidine taken up from blood into cells. To verify this hypothesis, we performed transcellular transport studies with a double transfectant composed of basolateral hOCT2 and apical hMATE1. We found that 1 μM cimetidine was taken up from the

TABLE 2
Comparison of affinity for hMATE1, hMATE2-K, and hOCT2 (rOCT2) of organic cations and various drugs excreted from kidney

Compounds	K_m or K_i Values for [^{14}C]TEA Uptake		Affinity for hOCT2 (rOCT2) from Previous Articles[b]	Comparison of Affinity	Effective Plasma Concentration[c]
	hMATE1	hMATE2-K			
	μM				μM
Organic cations					
TEA	380[a]	760[a]	48–270	MATE < OCT	
1-Methyl-4-phenylpyridinium	100[a]	110[a]	19–78	MATE < OCT	
Antidiabetic drug					
Metformin	667	6516	339–1700	MATE < OCT	4.1
Antiarrhythmic drugs					
Disopyramide	84	292	(64)	MATE < OCT	>4.4
Procainamide	217	178	50–58	MATE < OCT	11–52
Quinidine	29	23	(19)	MATE < OCT	6–18
Histamine H_1 receptor antagonist					
Cetirizine	371	818	No data		0.55
Histamine H_2 receptor antagonists					
Cimetidine	1.1	7.3	8.6–73	MATE > OCT	2.0–3.6
Famotidine	0.6	9.7	111–204	MATE > OCT	0.04
Ranitidine	25	25	40–265	MATE > OCT	0.28
Antiparkinsonian agents					
Amantadine	112	1167	20–28	MATE < OCT	1.6
Pramipexole	141	24	(17)	MATE < OCT	0.001
Talipexole	66	120	No data		0.002

[a] The K_m values obtained from a previous paper (Tanihara et al., 2007).
[b] The affinity for OCT2 obtained from previous work (Urakami et al., 2001; Ishiguro et al., 2005; Koepsell et al., 2007).
[c] The effective plasma concentration obtained from the data of Benet et al. (1996).

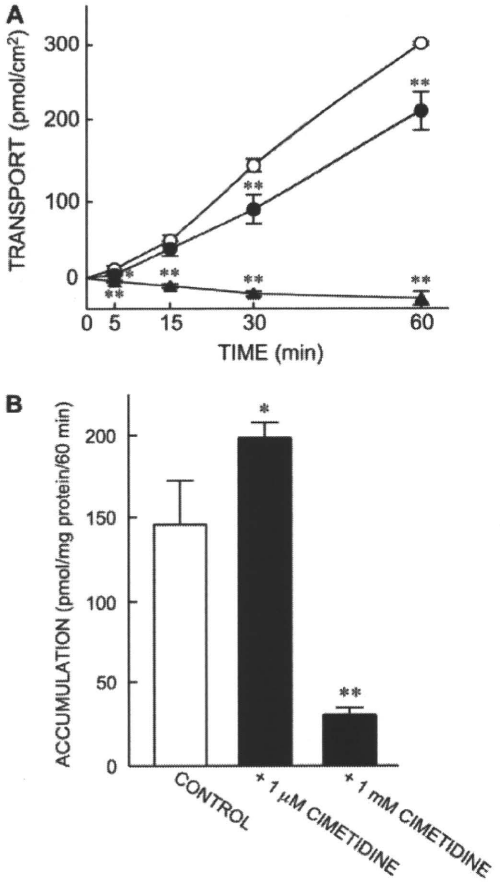

Fig. 4. Effects of cimetidine on transcellular transport (A) and intracellular accumulation (B) of [^{14}C]metformin by MDCK-hOCT2/hMATE1 cells. The cell monolayers were incubated at 37°C with 2 ml of incubation medium, pH 7.4, containing [^{14}C]metformin (10.6 μM) and D-[^{3}H]mannitol (0.079 μM) added to the basolateral side in the absence (Control, ○) or presence of either 1 μM cimetidine (●) or 1 mM cimetidine (▲), and 2 ml of nonradioactive incubation medium, pH 6.0, was added to the apical side. After the incubation, the radioactivity on the apical side and intracellular accumulation were measured. Transcellular transport of [^{14}C]metformin was calculated by subtracting the flux of [^{3}H]mannitol from the net flux of [^{14}C]metformin. After 60 min of incubation, the cell monolayers were washed twice with ice-cold incubation medium, and the radioactivity of solubilized cells was determined. Each point and column represent the mean ± S.D. for three monolayers. When error bars are not shown, they are smaller than the symbols. These figures are representative of two separate experiments. *, $P < 0.05$; **, $P < 0.01$, significantly different from control.

basolateral side without an inhibitory effect on metformin transport via hOCT2, and intracellular cimetidine inhibited the transport of metformin via hMATE1 (Figs. 4–6). These results suggest that hMATE1 is responsible for the drug interaction between cimetidine and metformin. In fact, it has been reported that cimetidine significantly increased the area under the curve of metformin by an average of 50% and reduced its renal clearance over 24 h by 27% in human subjects (Somogyi et al., 1987). Cimetidine has been shown to be an inhibitor of the active tubular secretion of many cationic drugs, including procainamide (Somogyi et al., 1983; Christian et al., 1984), *N*-acetylprocainamide (Somogyi et al., 1983), ranitidine (van Crugten et al., 1986), triamterene (Muirhead et al., 1986), pilsicainide (Shiga et al., 2000), and varenicline (Feng et al., 2008). These drug interactions could

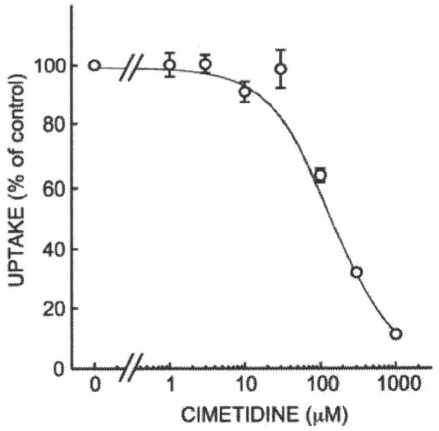

Fig. 5. Effects of cimetidine on [^{14}C]metformin uptake by HEK-hOCT2 cells. HEK-hOCT2 cells were preincubated with incubation medium, pH 7.4, for 10 min. The preincubation medium was removed, and the cells were incubated with 10.6 μM [^{14}C]metformin in the presence of cimetidine for 2 min at 37°C, pH 7.4. The radioactivity of solubilized cells was then measured. Each point represents the mean ± S.D. for three monolayers. This figure is representative of three separate experiments.

be partially mediated by hMATE1 at the apical membrane in the proximal tubules.

Recently, it was reported that the 808G>T polymorphism of hOCT2 is associated with a reduced tubular secretion clearance of metformin, and the inhibition by cimetidine also seemed to be dependent on this mutation (Wang et al., 2008). These results suggested that the drug interaction between cimetidine and metformin was affected by accumulation of metformin in the renal epithelial cells. This report would support our notion that the hMATE family plays an important role in the cimetidine-metformin interaction in vivo.

It has been reported that cisplatin, an anticancer platinum agent, was accumulated in the kidney via hOCT2 and induced nephrotoxicity. On the other hand, oxaliplatin was transported by hMATE2-K and hOCT2; therefore, its renal cellular concentration was lowered, suggesting that oxaliplatin did not induce nephrotoxicity (Yonezawa et al., 2006;

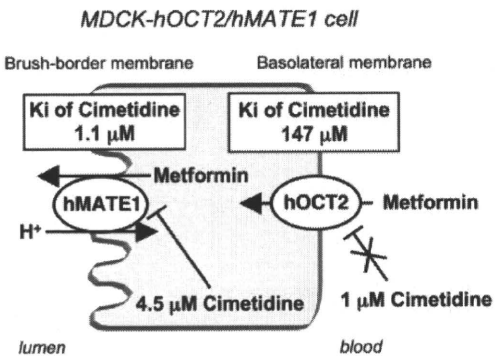

Fig. 6. Scheme of drug interaction between cimetidine and metformin in MDCK-hOCT2/hMATE1 cells. K_i values of cimetidine for hMATE1 and hOCT2 were calculated as 1.1 and 147 μM, respectively. When cimetidine at 1 μM was added to the basolateral side, intracellular concentration of cimetidine after 60 min incubation was calculated as 4.5 ± 0.4 μM. Considering K_i values and intracellular concentration of cimetidine, 1 μM cimetidine at the basolateral side did not inhibit metformin transport via hOCT2. However, intracellular cimetidine at 4.5 μM was enough to inhibit the metformin transport via hMATE1. These findings suggested that apical hMATE1 mainly contributed to the drug interaction between cimetidine and metformin.